

the
abdus salam
international centre for theoretical physics

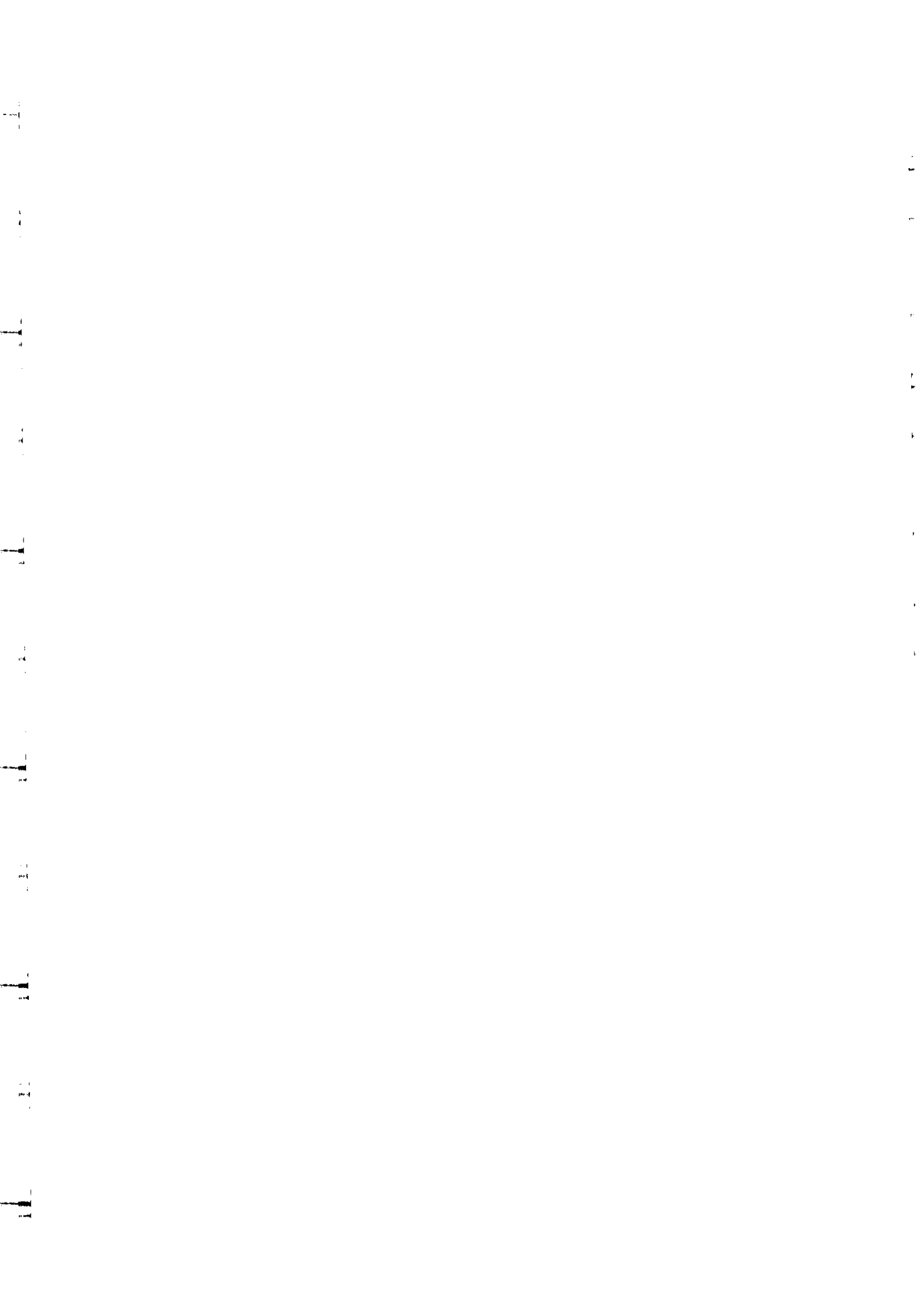
SMR.1135 - 15

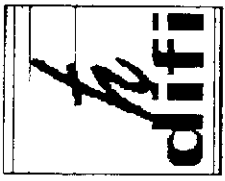
**THIRD WORKSHOP ON
THIN FILMS PHYSICS AND TECHNOLOGY
(8 - 24 MARCH 1999)
including
TOPICAL CONFERENCE ON
MICROSTRUCTURE AND SURFACE MORPHOLOGY
EVOLUTION IN THIN FILMS
(24 - 26 MARCH 1999)**

**"Effect of ion bombardment on the
evolution of surface morphology"**

**Ugo VALBUSA
Universita' degli Studi di Genova
Dipartimento di Fisica
Via Dodecaneso 33
16146 Genova
ITALY**

These are preliminary lecture notes, intended only for distribution to participants





U. Valbusa
INFN and

Physics Dept. University of Genova, Via Dodecaneso 33
16146 Genova Italy

Valbusa(a)fisica.unige.it

<http://www.fisica.unige.it/valbusa>



Ro
Co
Wi
SI





Introduction

- ultra-thin films
 - Epitaxial growth
 - Sputter Etching vs. Epitaxial growth
 - Surface morphology and Film growth
 - Nanostructuring thin films
- Sputter Etching
- Erosion and diffusion
 - Experiment



- Morphology of the film
 - Surface roughness
 - Scaling laws
 - Scaling laws vs growth
 - The case of metals Ag and Cu
- Applications
- Chemical reactions
 - Nanostructuring surfaces and films

ULTRATHIN FILMS

- thickness less than 10 atomic layers
- interest both from scientific and technological point of view
- They offer the possibility to obtain artificial materials with specific physical properties not observed in bulk materials



metastable crystalline phases
highly strained crystals

- A basic understanding of the nature of the growth process is a prerequisite for the design of films and multilayers with industrial applications in the areas of catalysis, electrochemistry, microelectronics and magneto-optical devices

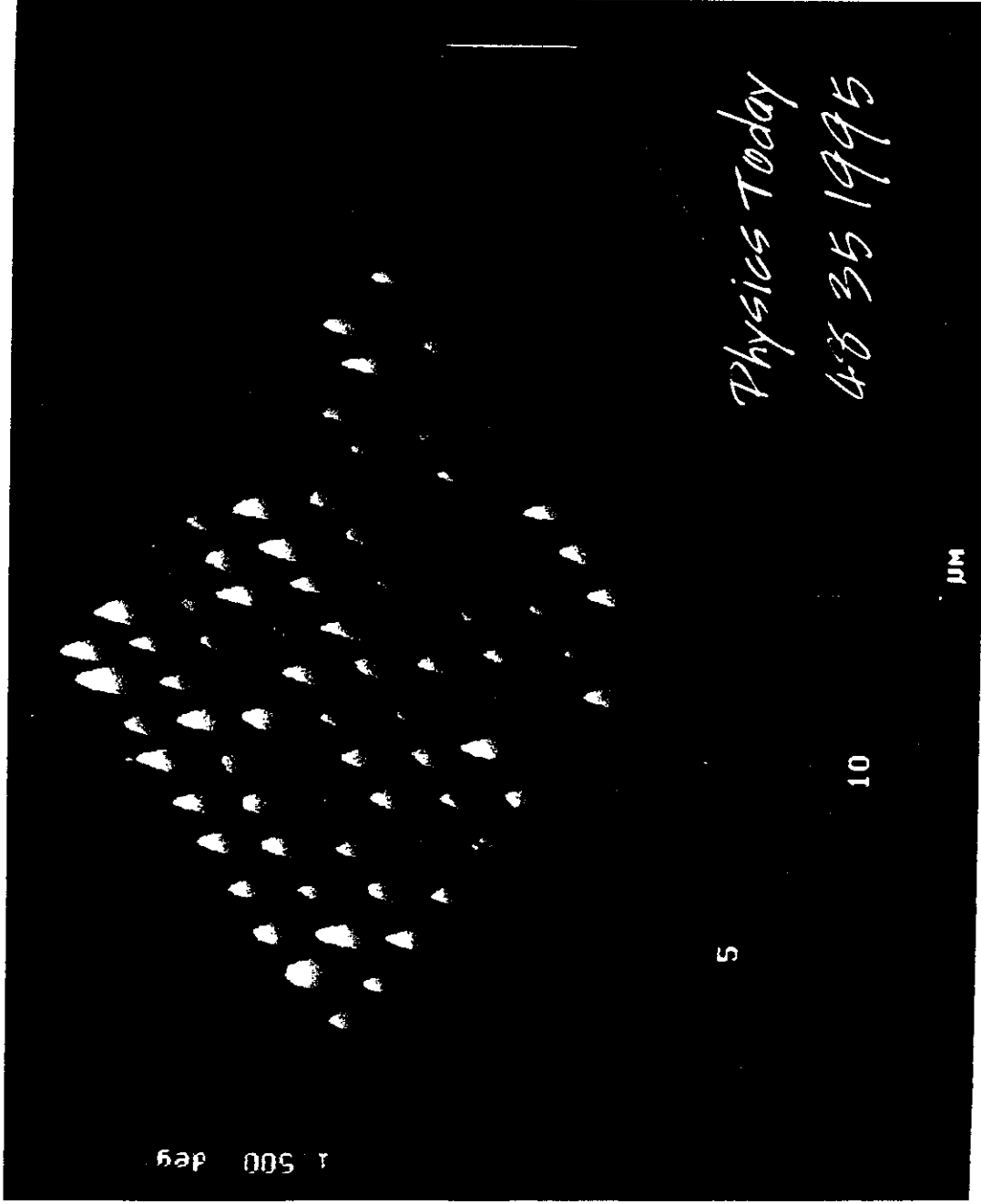
Magnetic Force

Image of rows of
bits on

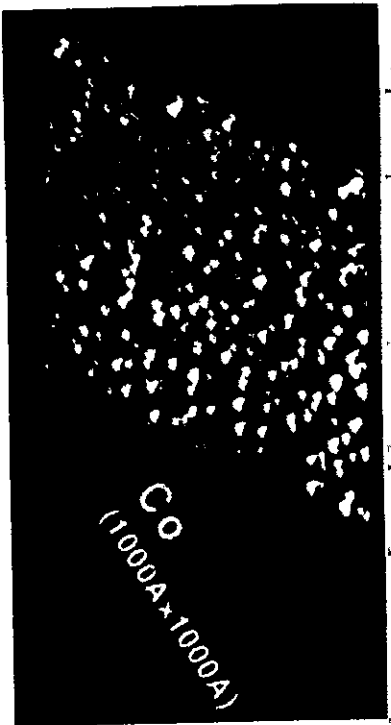
TbGdFeCo

magneto optical

medium produced
by 3M Corp.

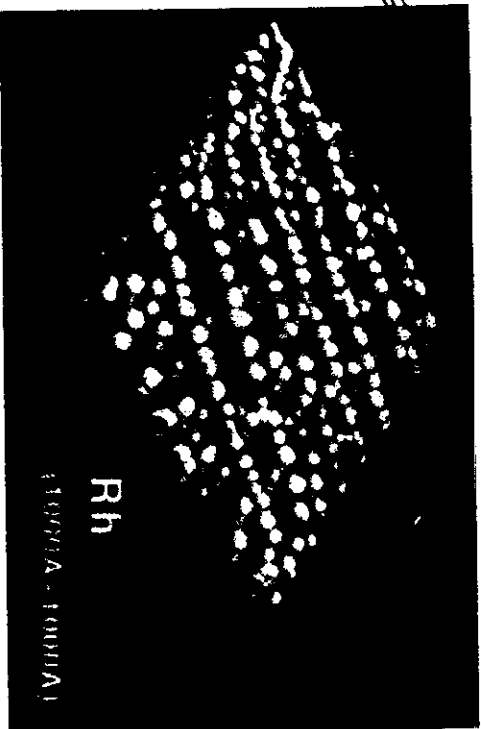


Bits were consistently written demonstrating the probing
of the local coercivity of the medium on a 100 nm scale

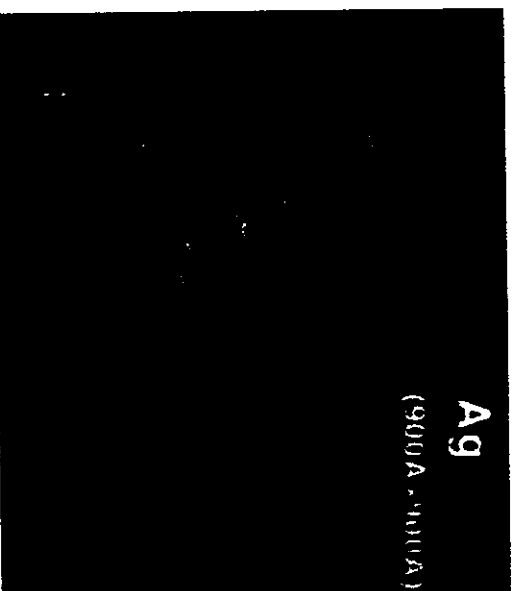


single-crystal surfaces of thin oxide
films supporting evaporated metal
aggregates

The three surfaces
contain similar
amount of
different metals



The metal-oxide
interaction strength
decreases from top
to the bottom



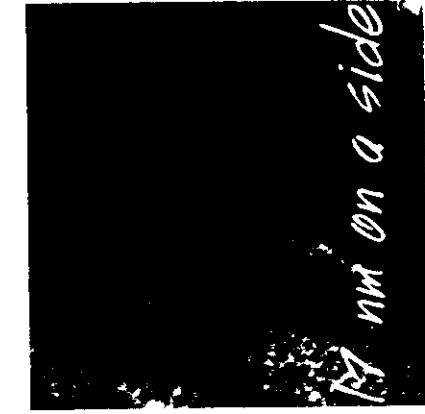
Ertl and Freund

Phys. Today 52 33 1999

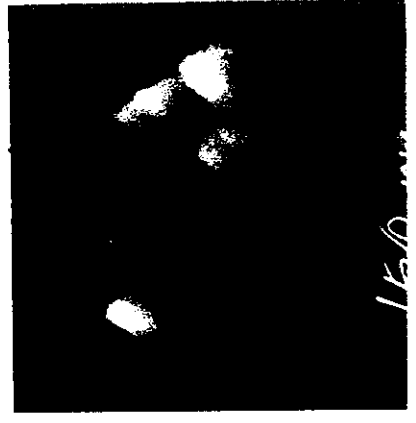


The oxygen-covered catalyst shows well-structured and ordered facets. A particle of silver becomes rough after oxidation of methanol

Schubert et al.
 Catal. Lett.
 33 305 1995



The dark areas are oxygen sites



After the silver particle catalyzes methanol, the topology changes

$$\Delta\gamma < 0$$

$$\Delta\gamma > 0$$

Frank-van der Merwe



Stranski-Krastanov



Volmer-Weber



Layer by layer FV

layer-plus-island SK

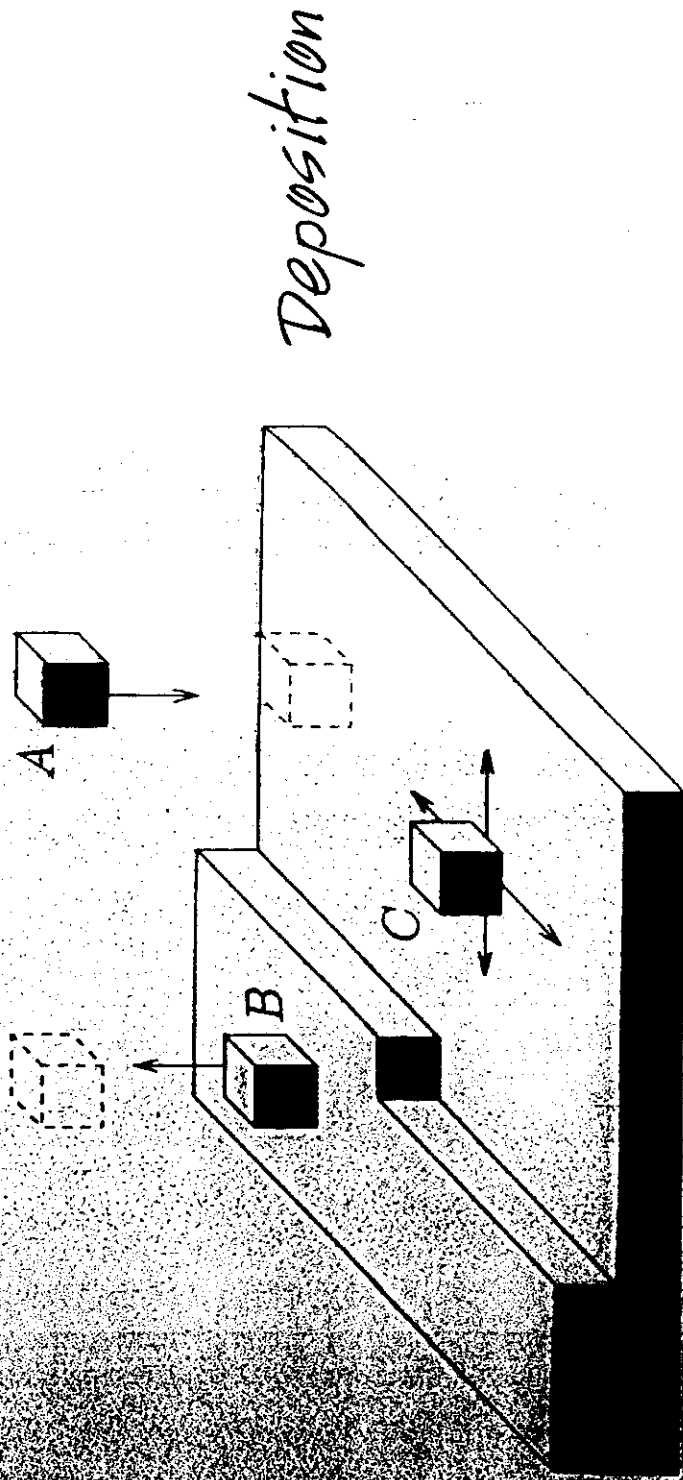
island growth VW

$$\Delta\gamma = \gamma_A + \gamma_{AS} - \gamma_S$$

γ is the surface free energy of the adatoms (A), substrate (S) and of the interface (AS).

There are two complementary approaches to
crystal growth:
atomistic in which the position of every atom is well
defined

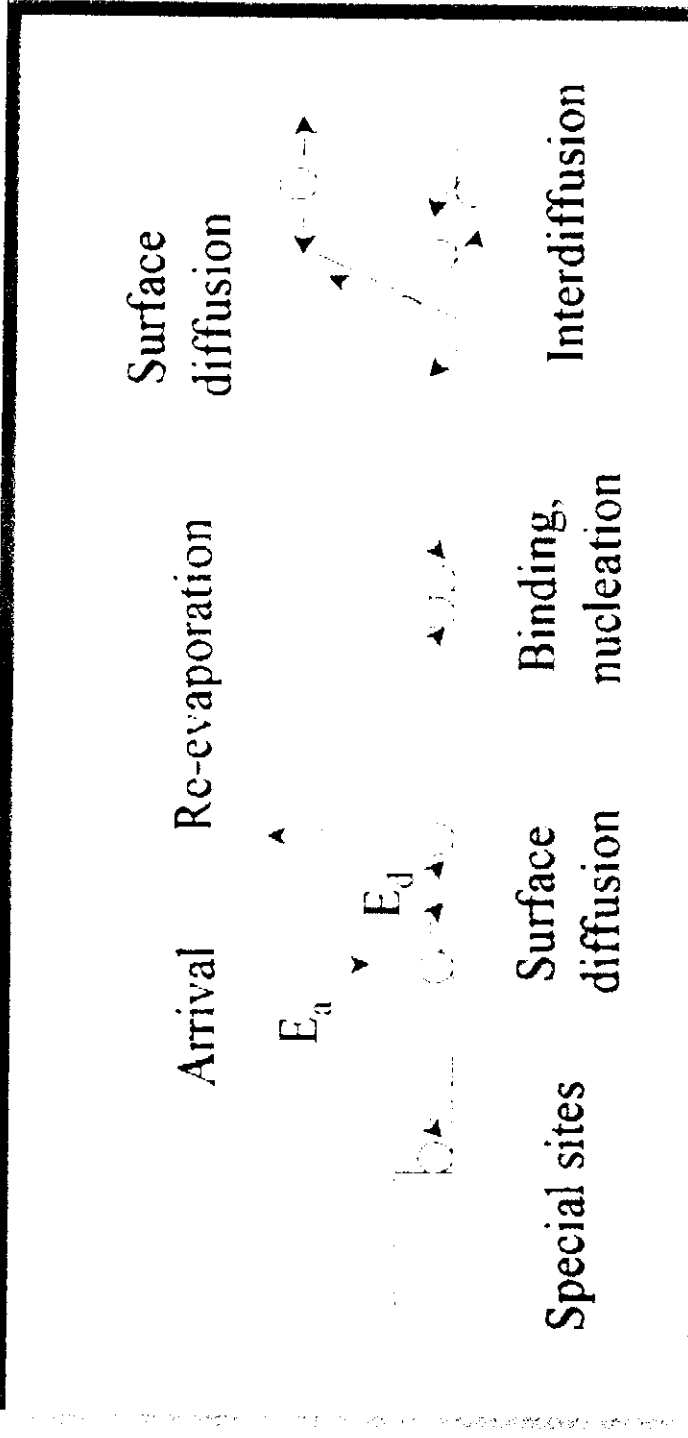
continuum in which the interface is view on a
coarse-grained scale where every atom is
averaged over a small volume containing
many atoms



UHV 10^{-10} mbar

Microscopic theory of nucleation

Elementary processes

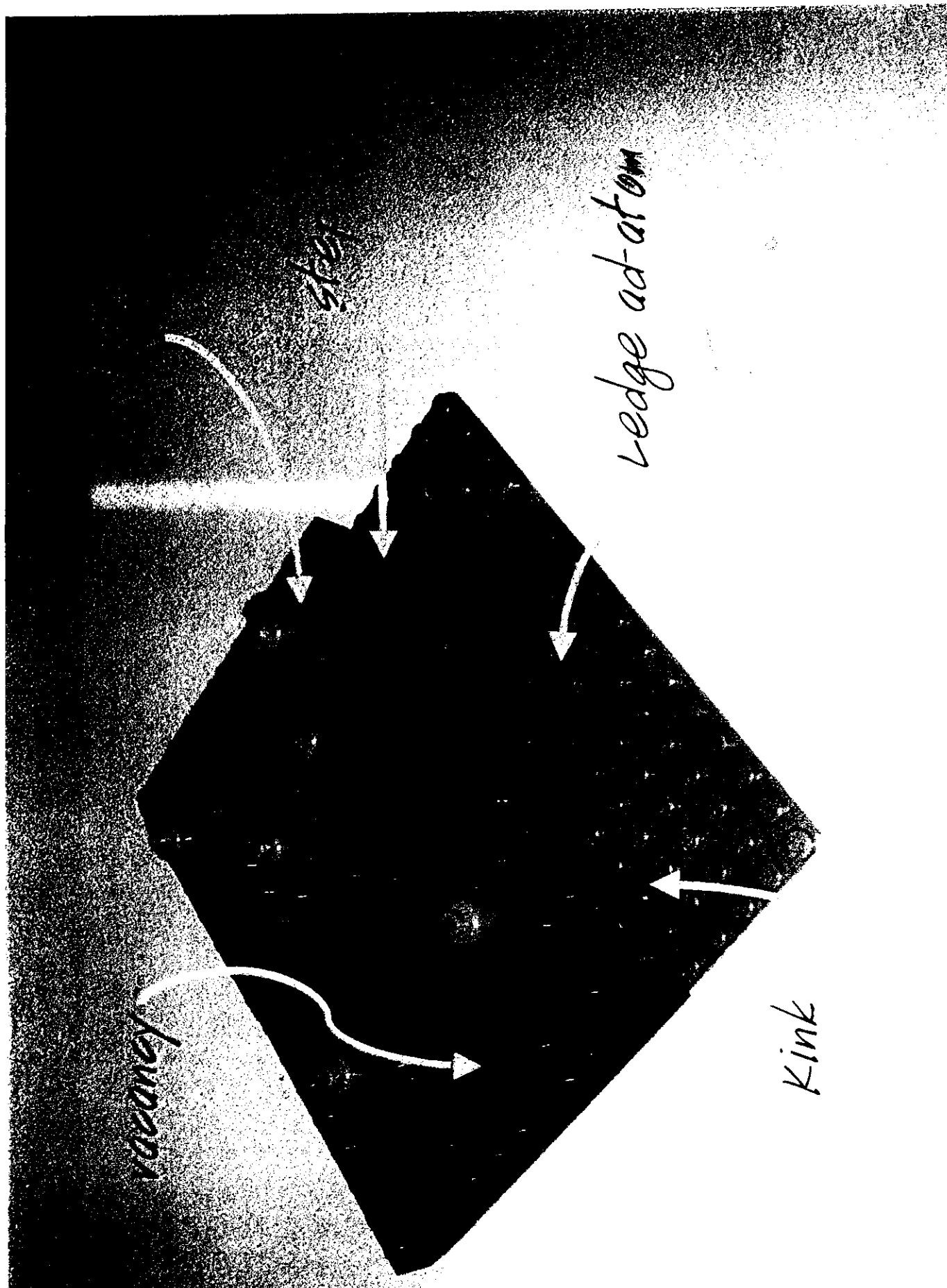


• The previous classification is based on thermodynamic properties of ad-atom-substrate system and is correct only if thermodynamic equilibrium is established.

• The film growth proceeds under conditions of thermodynamic equilibrium.

• The final structure and morphology of the film depends on many possible types of kinetic paths each with length which can be very different.

• Thermodynamic properties do not account for the microscopic surface morphology and consider the surface as ideal without crystalline defects, which at the contrary have an important role in the growth process.



steps

ledge ad-atom

Kink

vacancy

- Atoms arrive from the vapor at a rate

$$R = P / (2\pi m k T)^{1/2}$$

- The atoms areal density is

$$n(t) = R t$$

- The adsorption residence time

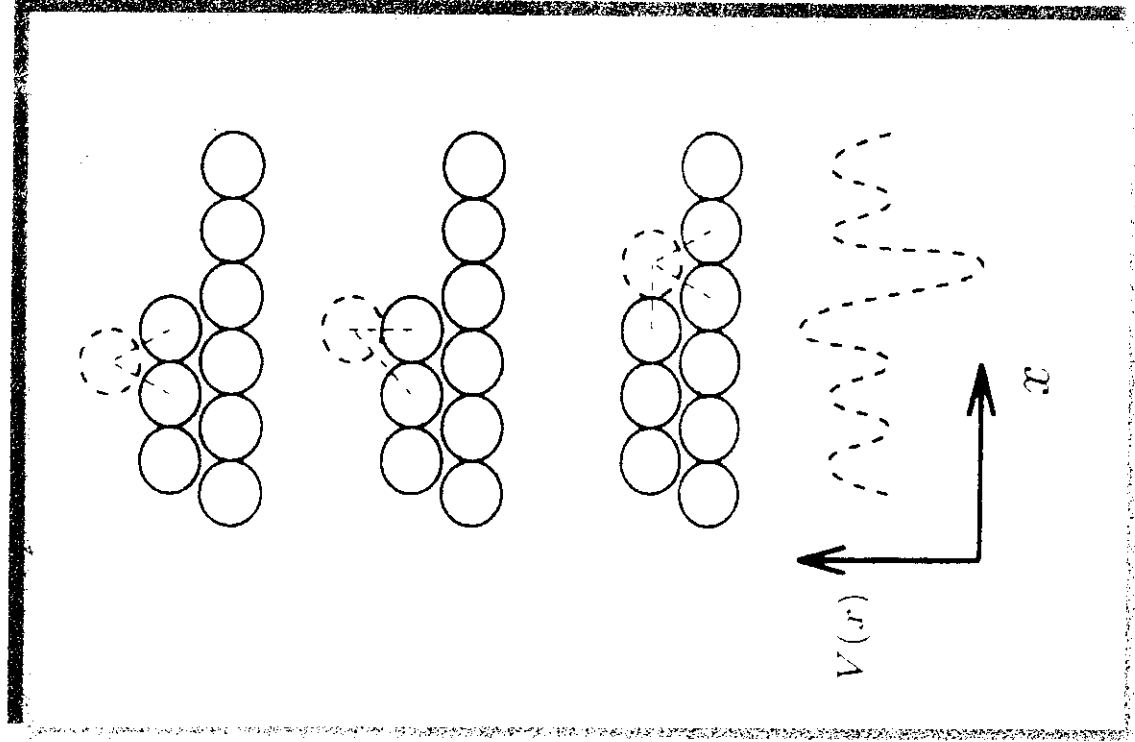
$$\tau_a^{-1} = \nu_a \exp(-E_a / kT)$$

$$\nu_a = 1 - 10^{13} \text{ Hz}$$

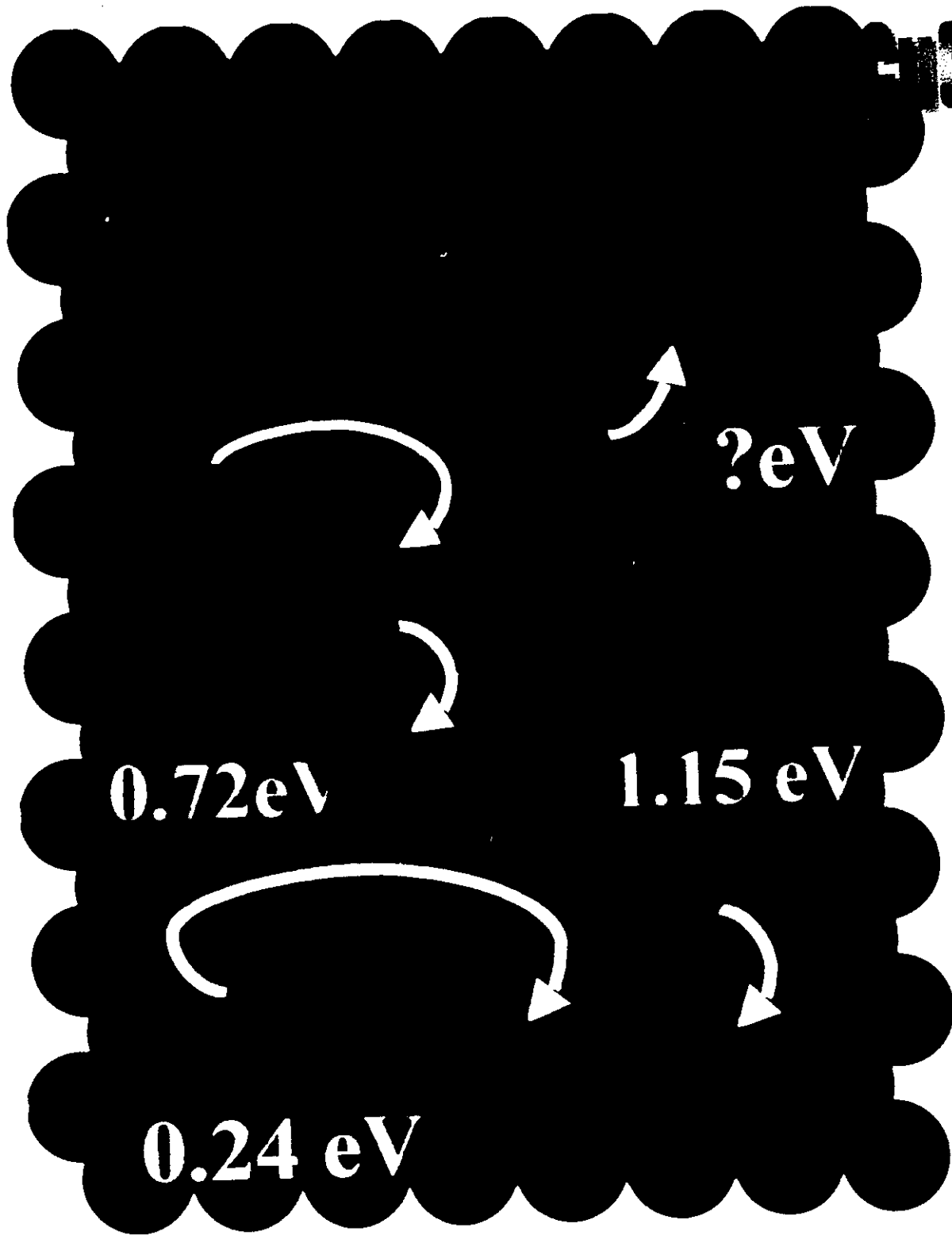
- What happens if the atom diffuses on the island and approaches its edge from above?
- There is an additional potential barrier at the edge of the island that atom must pass in order to jump off \therefore the probability of its being reflected is higher than the probability of its jumping off.

SCHWOBEL barrier

Diffusion bias

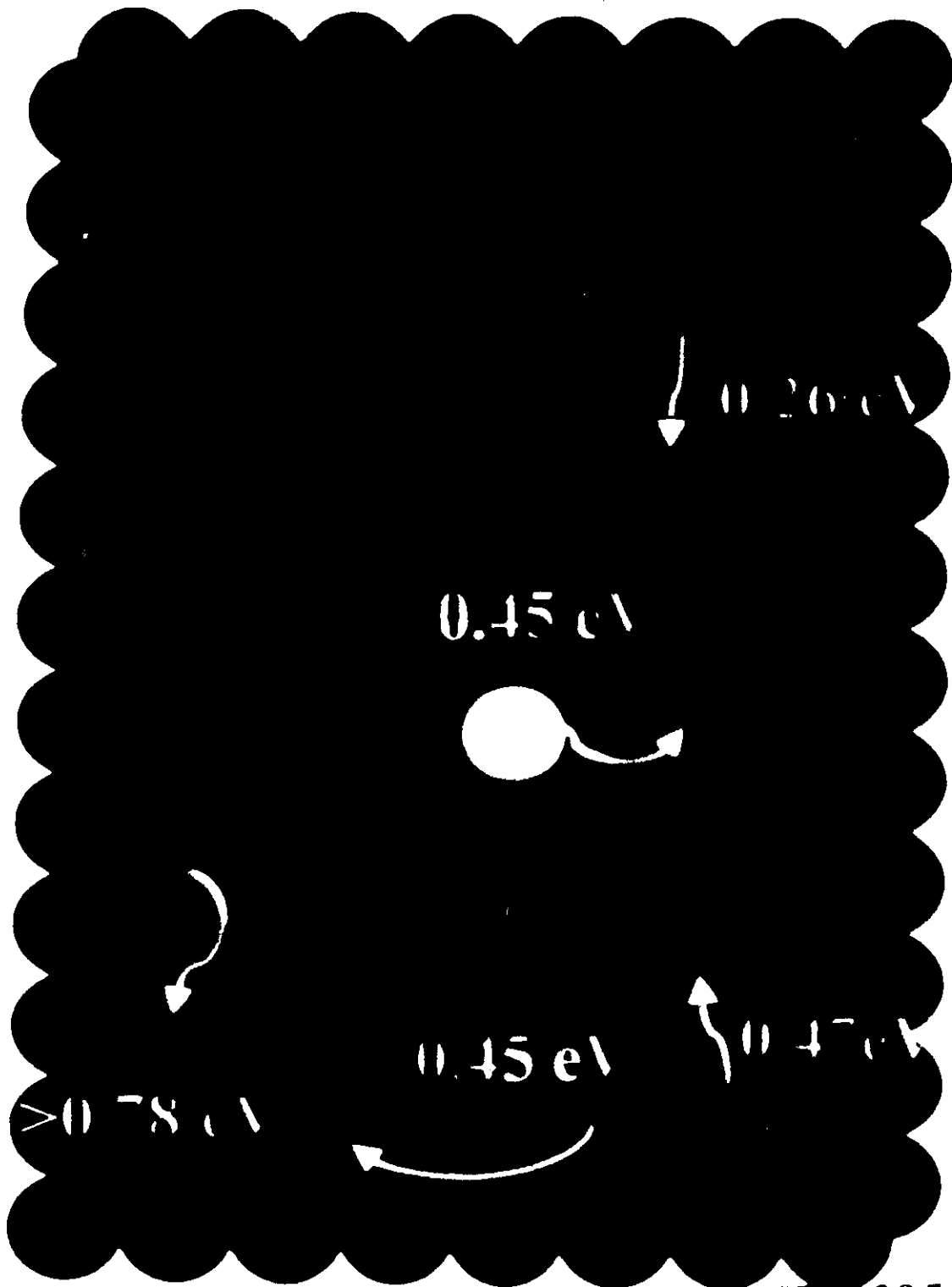


(110)



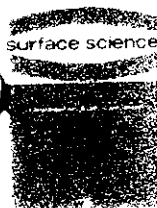
Karimi et al 5364 52 1995.

PHYSICAL REVIEW
B



Scheffler et al. 77, 1095 (1996)

Nelson et al. 295,462 (1993)



Desorption

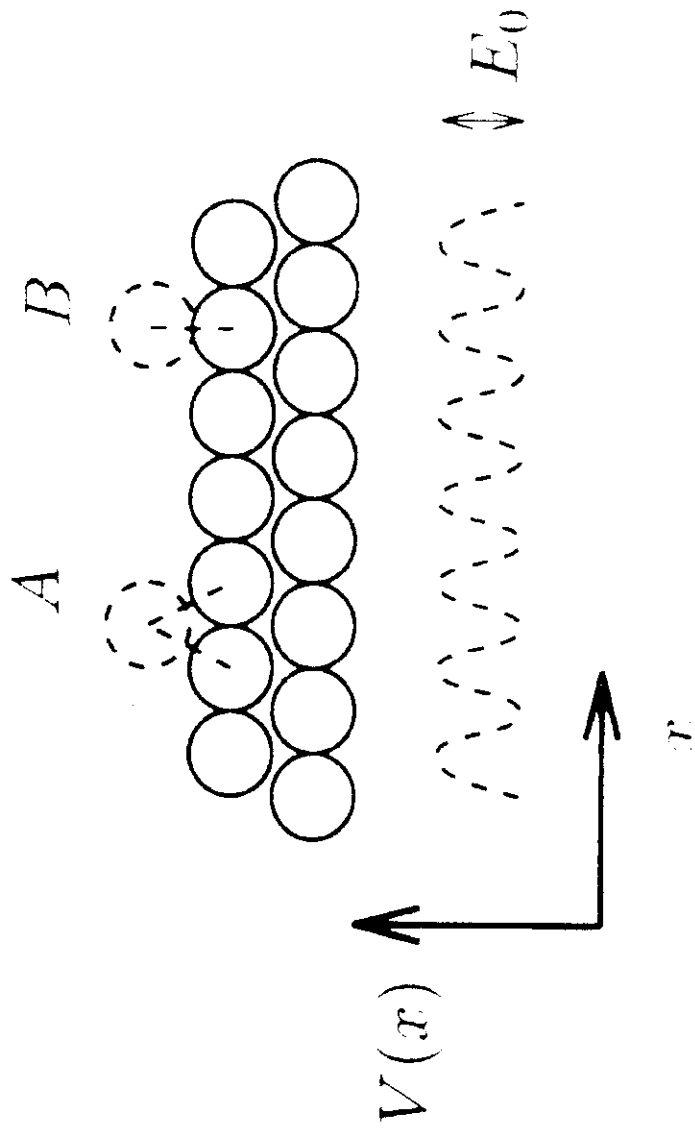
- The desorption probability depends on how strongly the atom is bonded to the crystal surface.
- Comparison among desorption time and time scale set by the deposition process

$$\tau = \tau_0 \exp(E_{\text{des}} / kT)$$

$$\tau_0 \approx 10^{-10} \text{ sec}$$

For Ga on GaAs (111) $E_{\text{des}} = 2.5 \text{ eV}$

At 850 K predicts that the lifetime of the deposited molecule is 2 sec.



• The diffusion constant is given by

$$D = \frac{1}{4} v_d^2 \exp(-E_d/kT) \quad v_d \text{ somewhat less than } v_a$$

where a is the jump distance of the order of the unit cell

Conclusions

- High T the diffusion length λ is very large. Atoms can find terraces or steps where they can stick
- Lowering T , λ decreases and islands will nucleate on the top of the existing islands as well
- lowering T still further, λ becomes very short. Only deposition determines the growth. The material becomes amorphous with a rough surface

Frank-van der Merwe

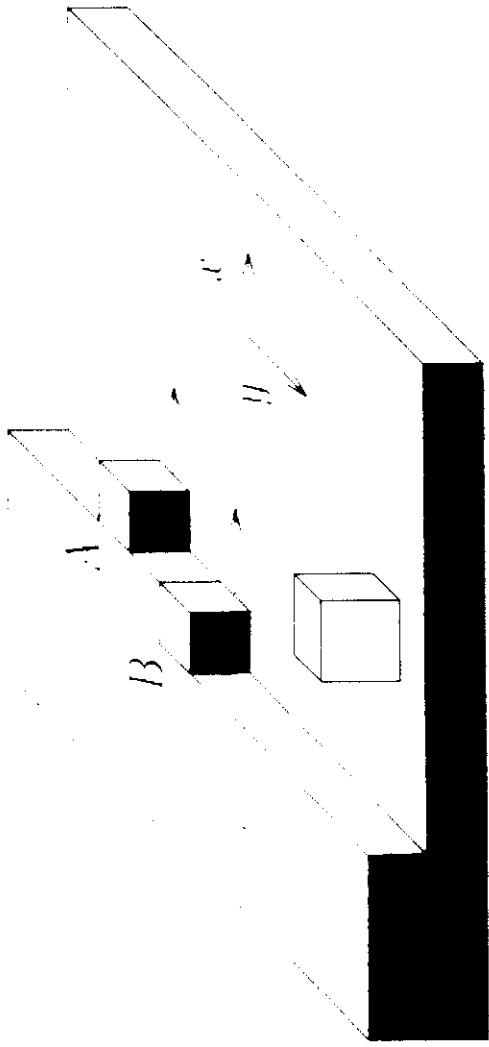


Stranski-Krastanov



Volmer-Weber



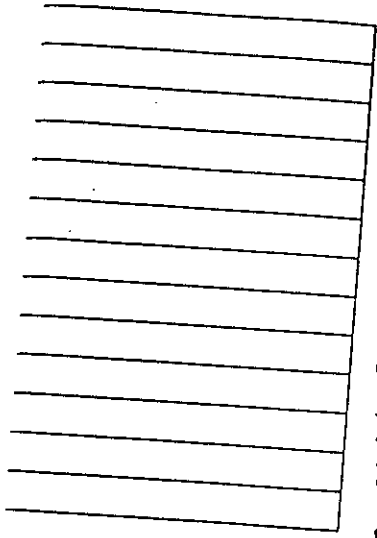


The probability that the atom B or A breaks the bond with an atom on the edge of the island is much

smaller than the characteristic diffusion probability of an atom on the surface

$$\approx \exp(-E_d + E_b) / kT$$

If $E_b = 1$ eV at 600 K this probability is 10^6 times smaller than the characteristic diffusion probability of an atom.



- The rms displacement of the adatom from the arrival time before

evaporation is

$$x = (D \tau_0)^{1/2} = a / 2 (V_d / V_a)^{1/2} \exp((E_a - E_d) / 2kT)$$

- In their migration over the surface the adatoms will encounter other atoms and form small aggregates which they may grow forming 2 or 3 dimensional islands.
- Special sites such as surface vacancies or steps may act as adatoms traps
- More complex processes can occur

Continuum approach

$$\frac{\partial h}{\partial t} = F(h, \vec{x}, t)$$

$$\frac{\partial h}{\partial t} = -\vec{\nabla} \cdot \vec{J}(\vec{x}, t)$$

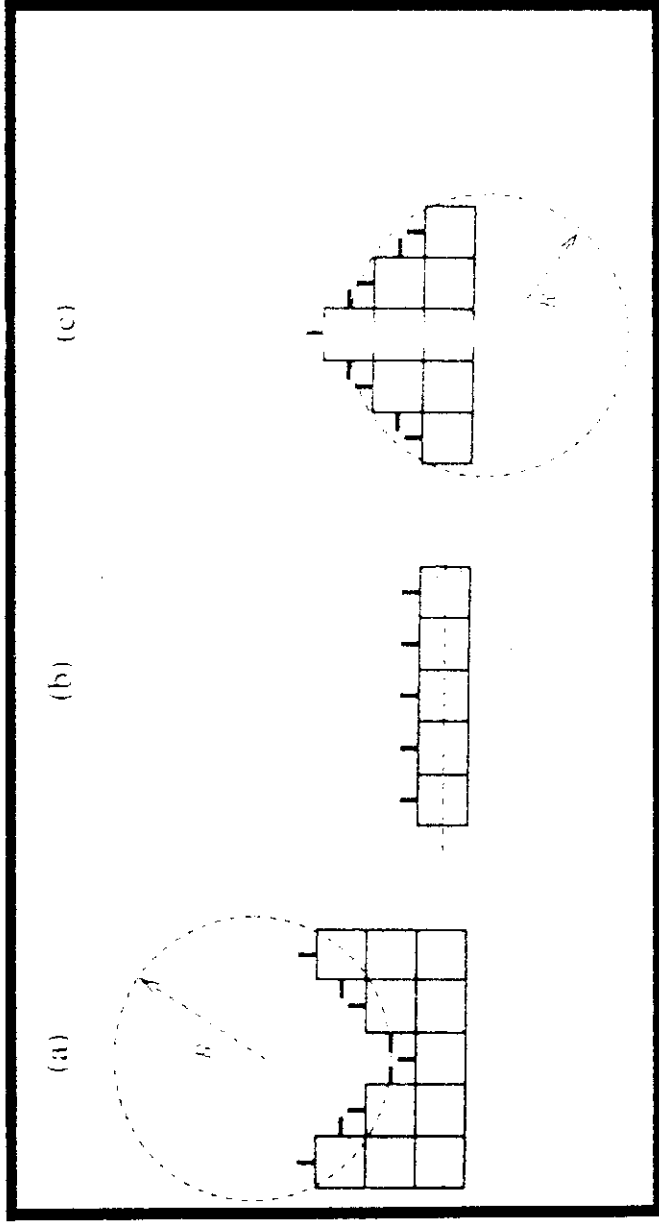
$$\vec{J}(\vec{x}, t) \propto -\vec{\nabla} \mu(\vec{x}, t)$$

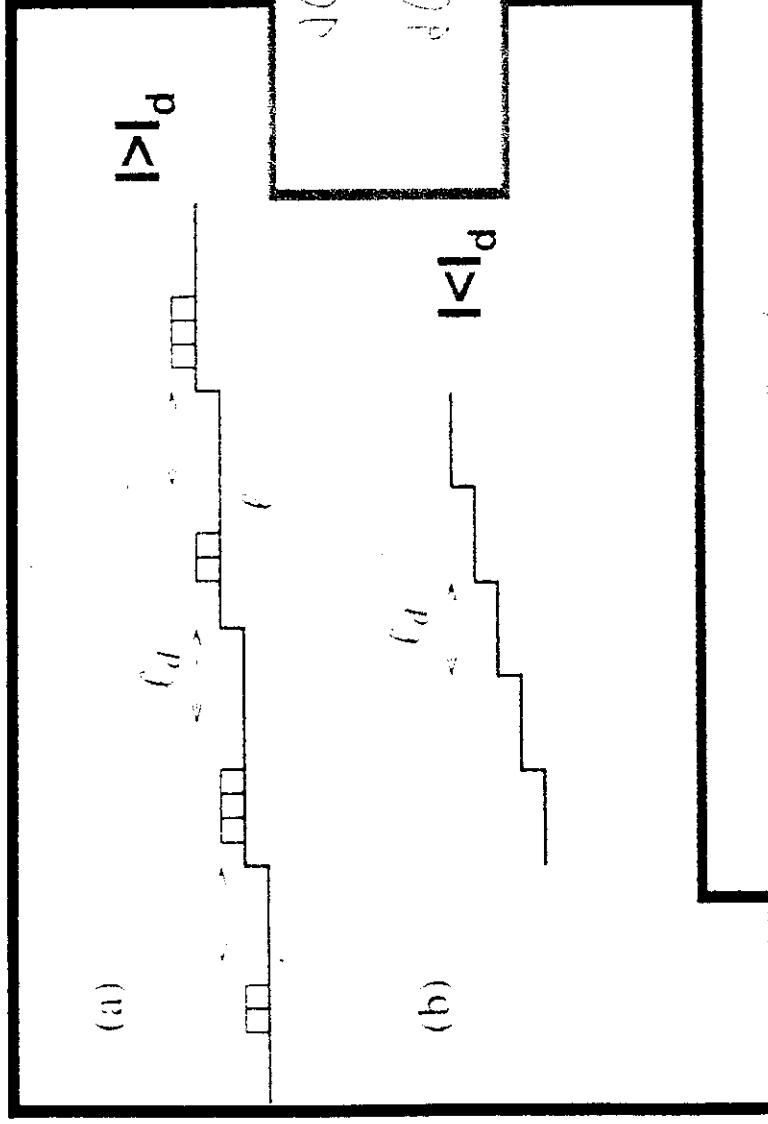
$$\frac{\partial h}{\partial t} = -k \nabla^4 h$$

F is the flux of the incoming particles
 η reflects the random fluctuations in the
deposition process $\langle \eta(x,t) \rangle = 0$

$$\frac{\partial h}{\partial t} = -k \nabla^4 h + F + \eta(\vec{x}, t)$$

$$\mu(\vec{x}_i^t) \propto -\nabla^2 h(\vec{x}_i^t)$$





$$d(m) \sim F l_d^2 m \quad l_d$$

$$d(m) \sim F e \sim \frac{F}{m} \quad e \ll e_d$$

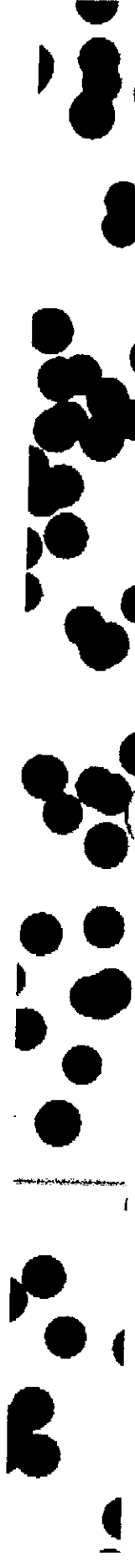
$$d(m) \sim F l_d^2 \left(\frac{m}{l_d} \right)^2$$

$$\frac{\partial h}{\partial t} = -\Delta \left(\frac{\Delta^2 h}{1 + |\Delta^2 h|^2} \right) - k \Delta^4 h + \eta(\vec{x}, t)$$

$$|\vec{v}_h| \ll 1$$

$$v \left(\frac{\vec{v}_h}{1 + (\vec{v}_h)^2} \right) \approx \vec{v}_h + \vec{v}^2 (\vec{v}_h)^2$$

$$\partial_t \vec{h} \approx -\vec{v}_h^2 \Delta + \vec{v}^2 (\vec{v}_h)^2 - k \vec{v}_h^4 + \eta (\vec{x}_i + t)$$



Epitaxial growth

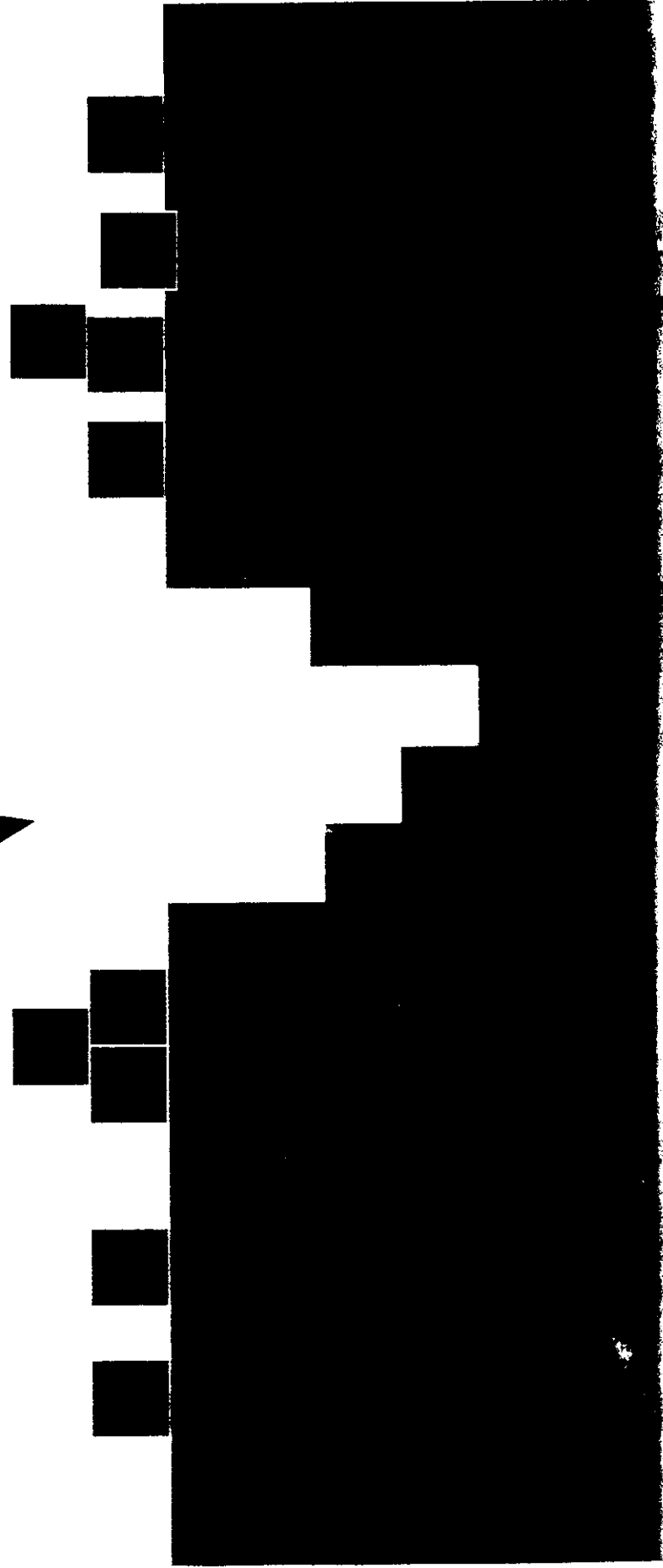
- Temperature of both source and substrate
- Pressure and nature of residual gas
- Rate of deposition of condensing atoms
- Surface mobility of deposit atoms
- Nature of the substrate (amorphous polycrystalline or mono-crystalline)



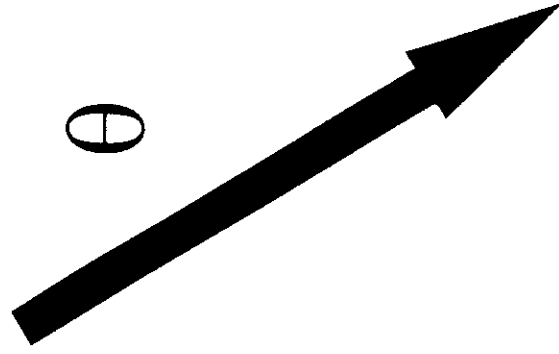
SPUTTER ETCHING



ion beam



sputter Etching



ion beam

- Ion Energy
- Ion flux
- Ion fluence
- azimuthal angle
- incidence angle θ

- polycrystalline
- single crystal
- Amorphous

- Ion Energy E is of the order of few keV
- Ion flux Φ is given by the gun current divided by the illuminated area
- Ion fluence Ψ is given by Φ times the time of ion bombardment $\Psi = \Phi t$
- azimuthal angle Φ defines the surface orientation respect to the ion beam
- incidence angle θ

Ion Bombardment

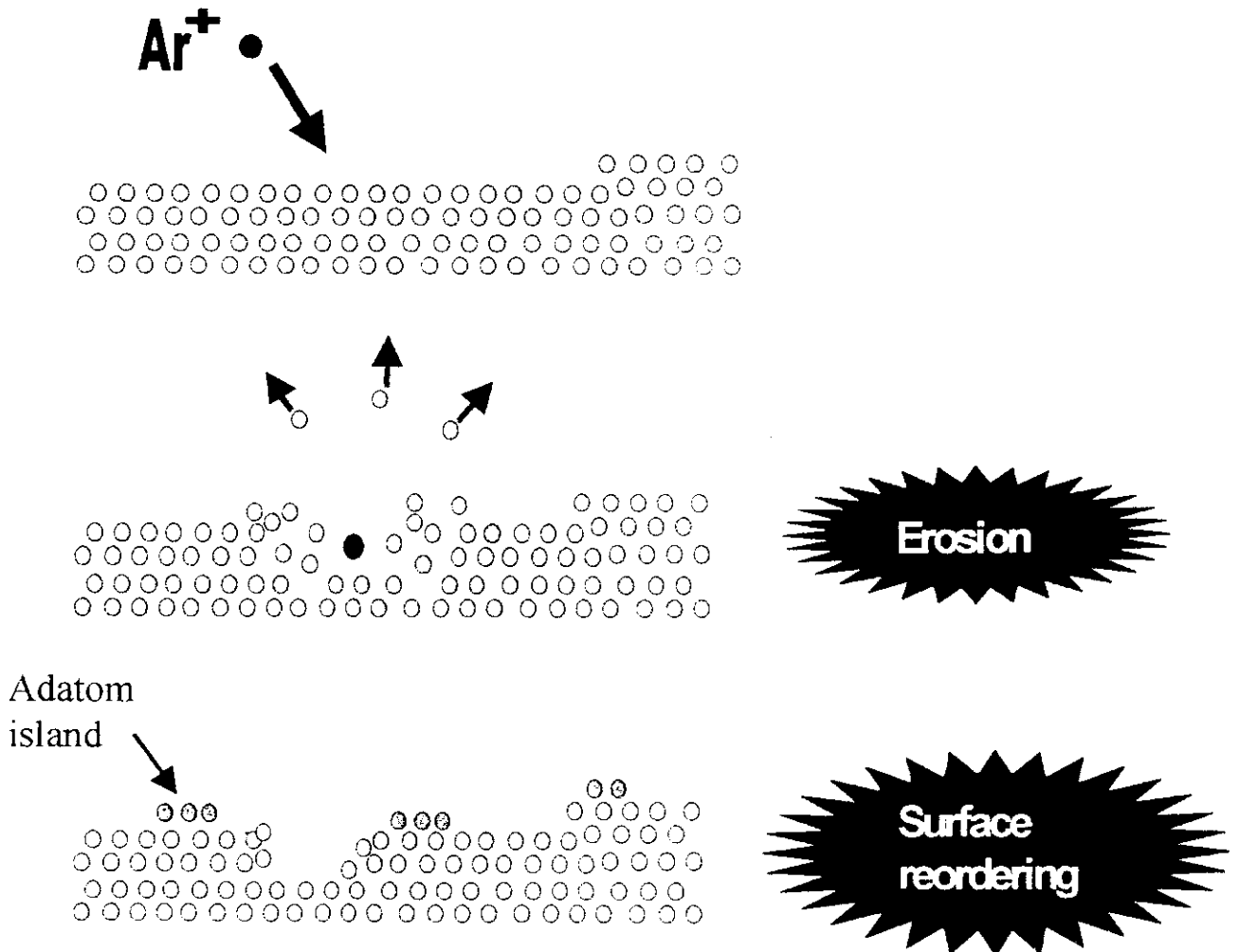
STM Image

Black spots = craters

White spots = adatom islands



Model



Ag(001)

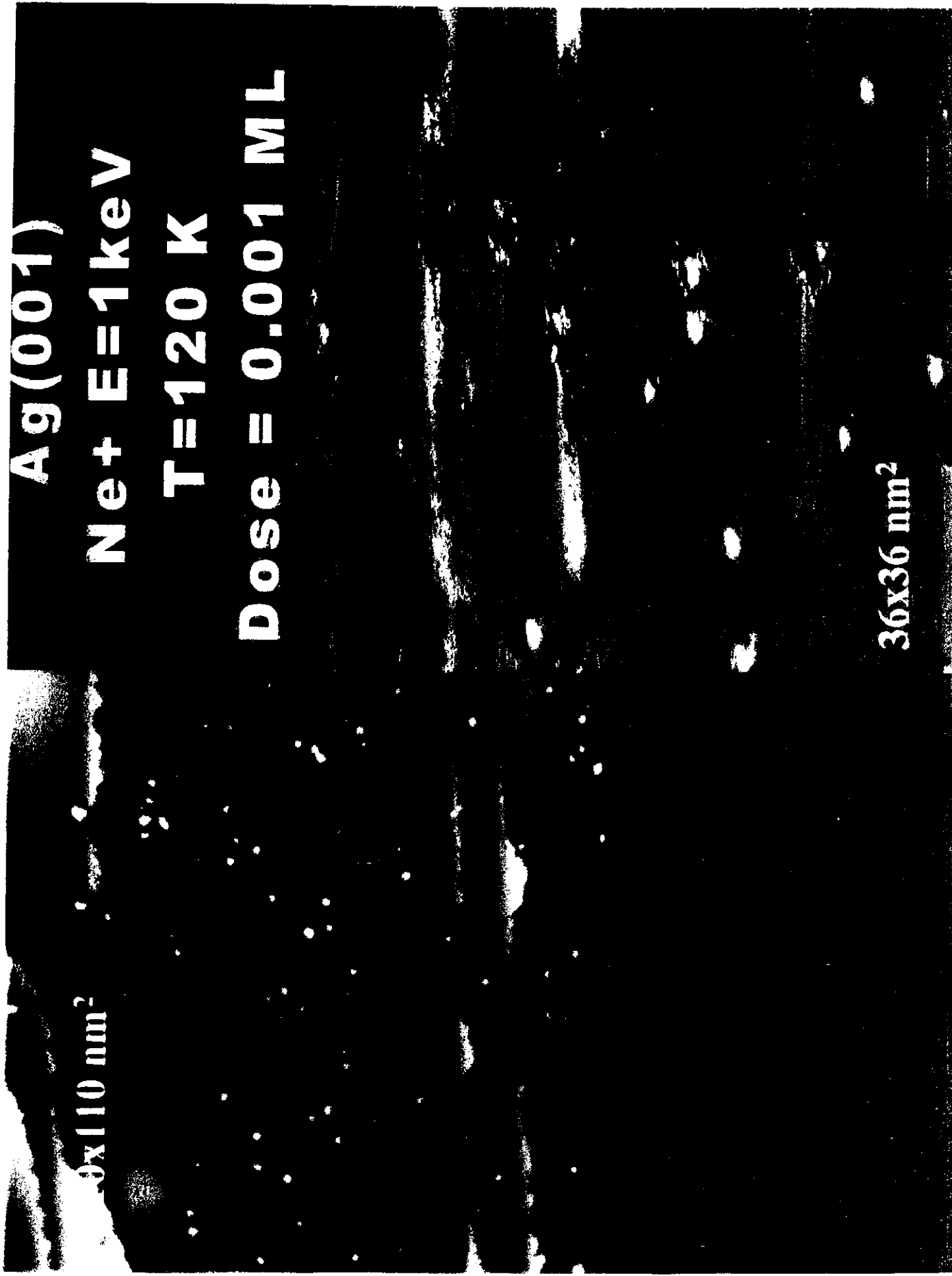
Ne+ E=1keV

T=120 K

Dose = 0.001 ML

36x36 nm²

10x110 nm²



44x44 nm



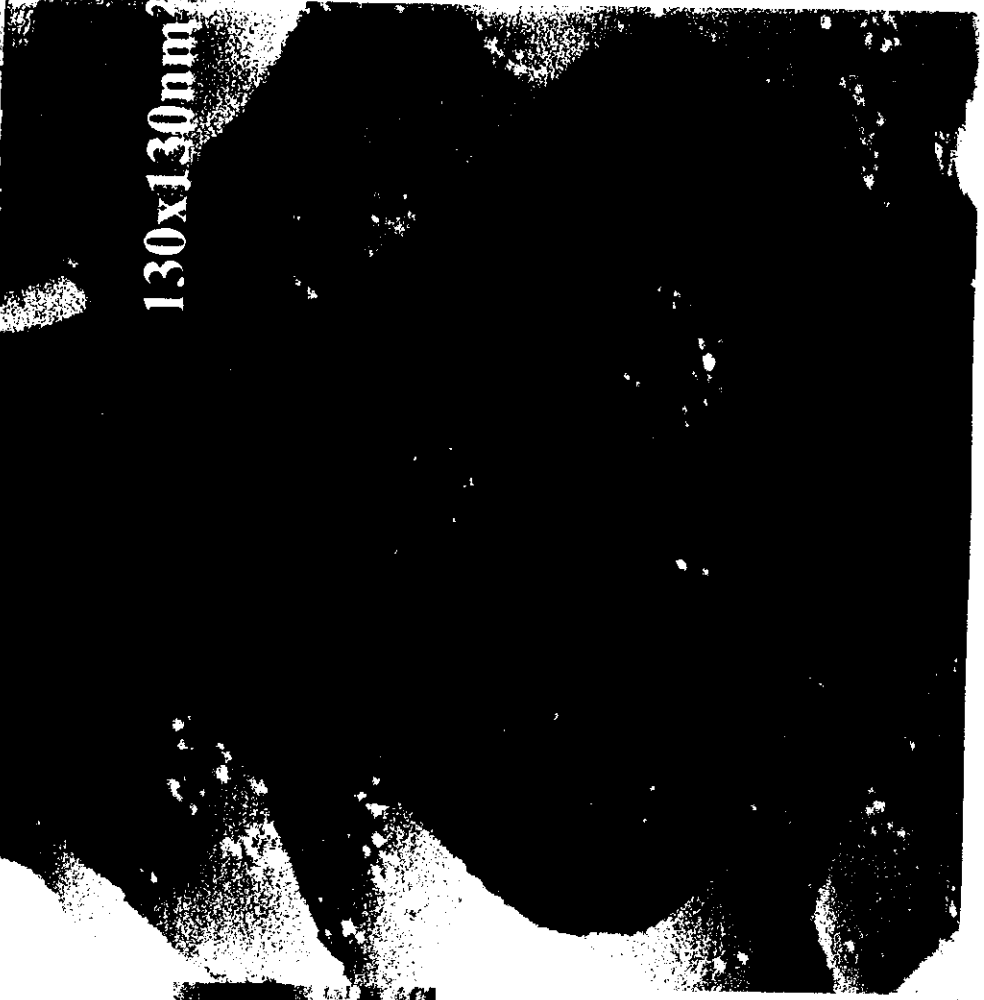
Ag(001)

Art. E=1keV

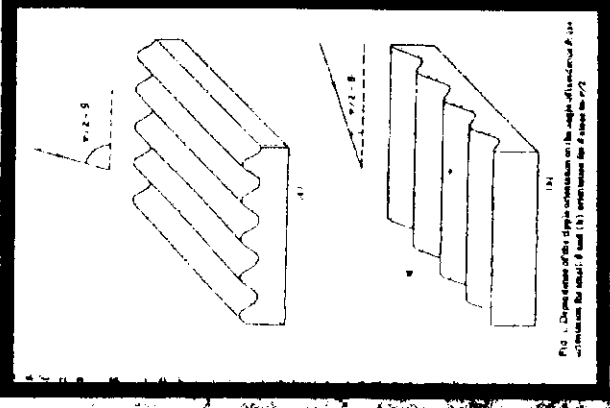
T=120 K

Dose=0.001 MI

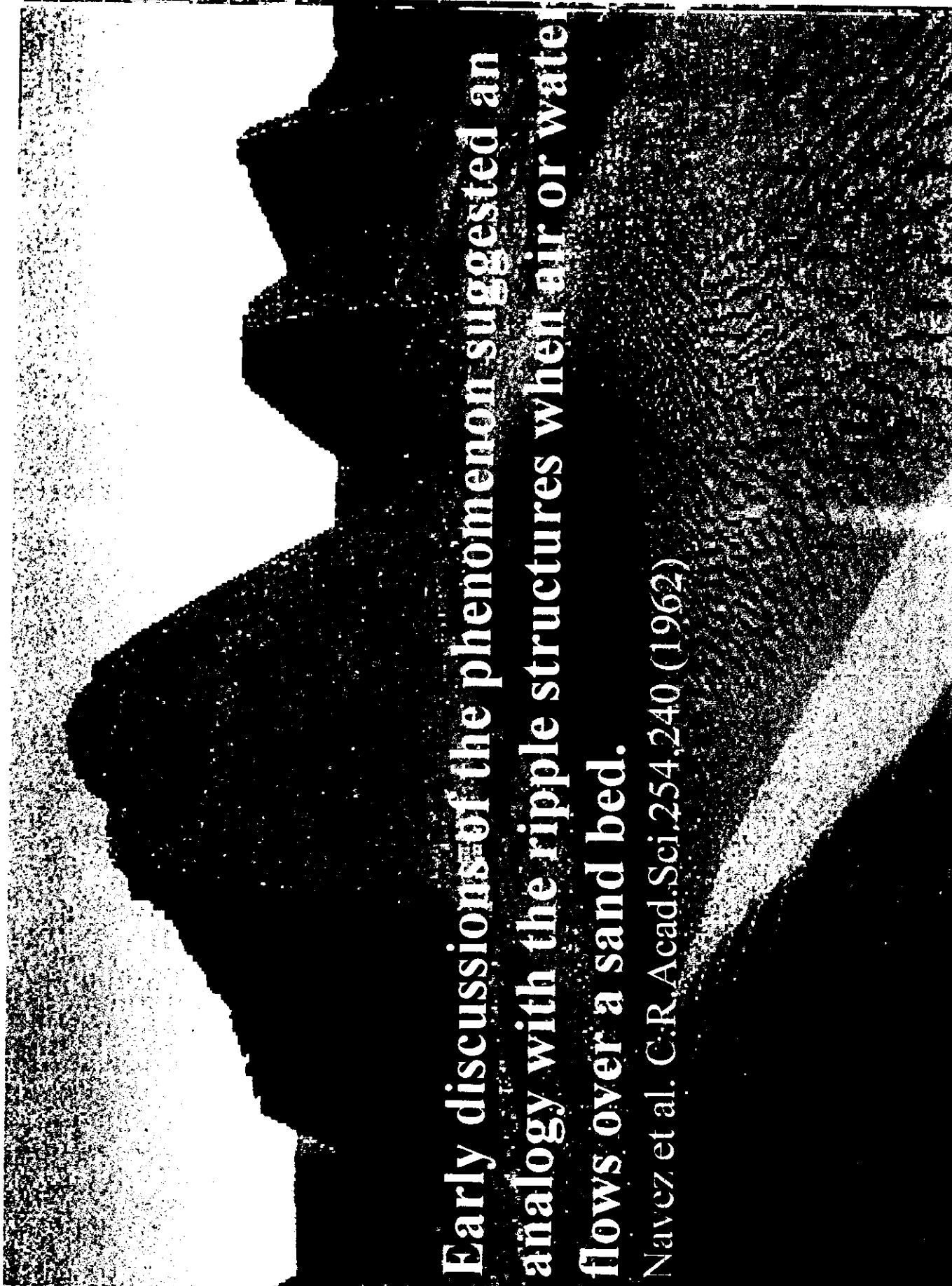
130x130nm



Off-normal incidence ion bombardment often produces periodic height modulations on the surface of amorphous solids



For the wave vector of the modulation k is // to the component of the ion beam in the surface plane
For k is perpendicular.
For one finds an interlocking grid of hillocks and depressions



Early discussions of the phenomenon suggested an analogy with the ripple structures when air or water flows over a sand bed.

Navez et al. C.R. Acad. Sci. 254, 240 (1962)

A much better analogy is found in the sandblasting of solids (Carter et al. Rad. Eff. 33, 65 (1977)). When a solid surface is eroded by a stream of of abrasive particles a regular ripple pattern is created with $k \parallel$ to the surface component of the incident stream.

The wavelength of the ripple formed by sandblasting is comparable to the distance over which a single particle is in contact with the surface.

The wavelength of the ripples formed by ion sputtering can be two orders of magnitude larger than the surface component of the ion range

Glass

MM. M. NAVEZ, C. SELLA et M^{lle} D. CHAPEROT
PLANCHE I.

1962

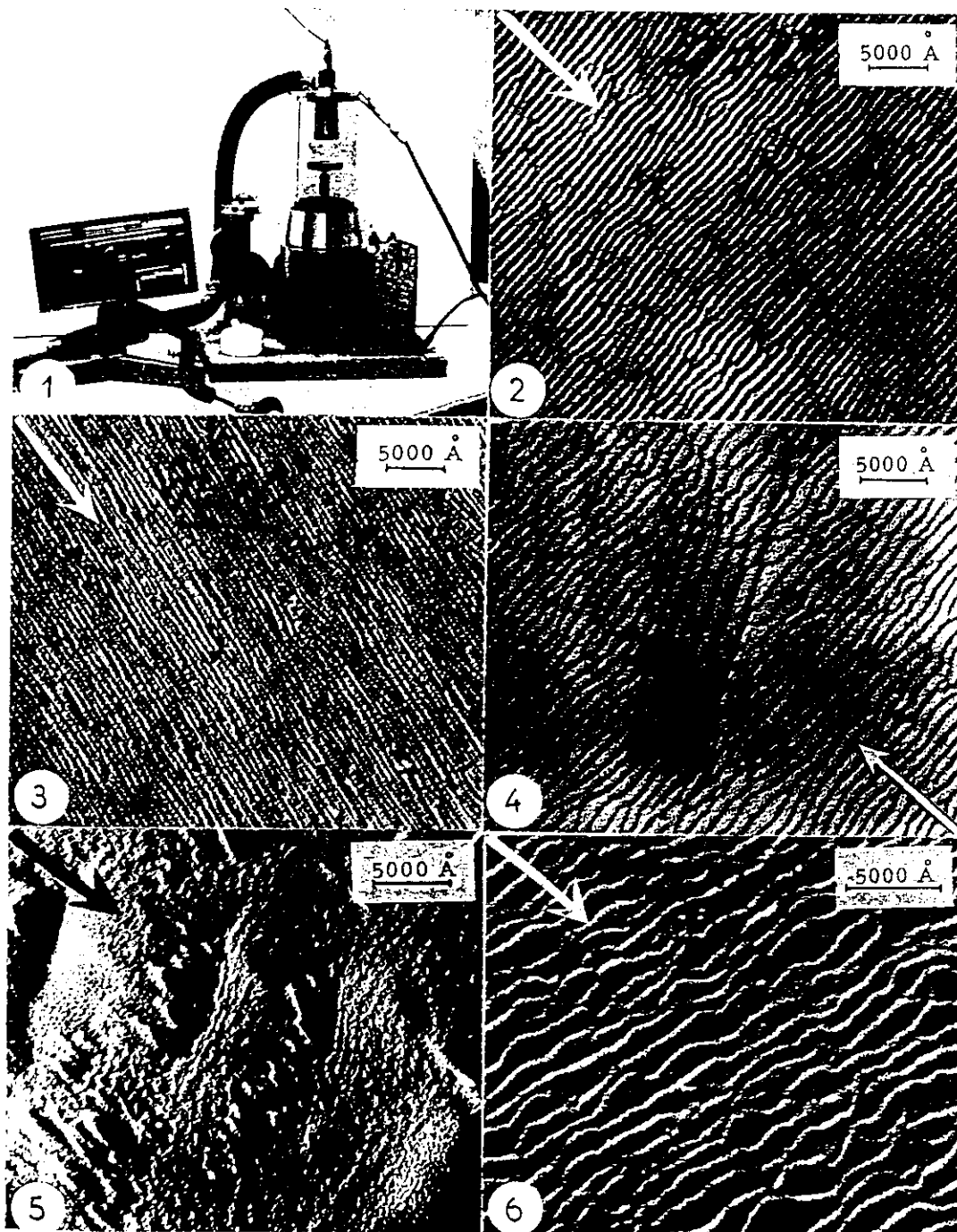
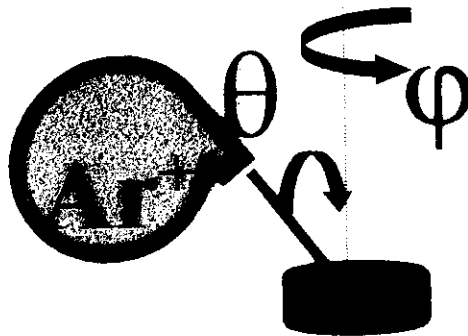


Fig. 1. — Canon à ions.

Fig. 1 à 6. — Surfaces de verre bombardées sous 10° (fig. 2),
sous 30° (fig. 6), sous 45° (fig. 4 et 5) et sous 60° (fig. 3).
(Les flèches indiquent la direction du faisceau ionique.)

Ion sputtering develops surface morphologies which are either **RIPPLE** (periodic) or **ROUGH** (non periodic)



The evolution of surface morphology during sputtering is the result of a balance between roughening and smoothing processes. Stochastic addition or removal of material tends to roughen the surface, while transport driven by surface energy minimization tends to smoothen the surface.

Theory of ripple topography induced by ion bombardment

R. Mark Bradley

Department of Physics, Colorado State University, Fort Collins, Colorado 80523

James M. E. Harper

IBM T. J. Watson Research Center, Yorktown Heights, New York 10598

(Received 16 July 1987; accepted 24 January 1988)

When an amorphous solid is etched by an off-normal incidence ion beam, a ripple topography often results. A theory explaining the origin of these waves is presented. For incidence angles close to the normal, we find that the ripple wave vector is parallel to the surface component of the beam direction, provided that longitudinal straggling of the beam is not too large. The ripple orientation is rotated by 90° when the beam is close to grazing incidence. The wavelength given by the theory varies as $\lambda \sim (fT)^{-1/2} \exp(-\Delta E/2k_B T)$ for high temperatures T and low fluxes f , where ΔE is the activation energy for surface self-diffusion. The predicted magnitude of the wavelength is in reasonable accord with experiments in this regime.

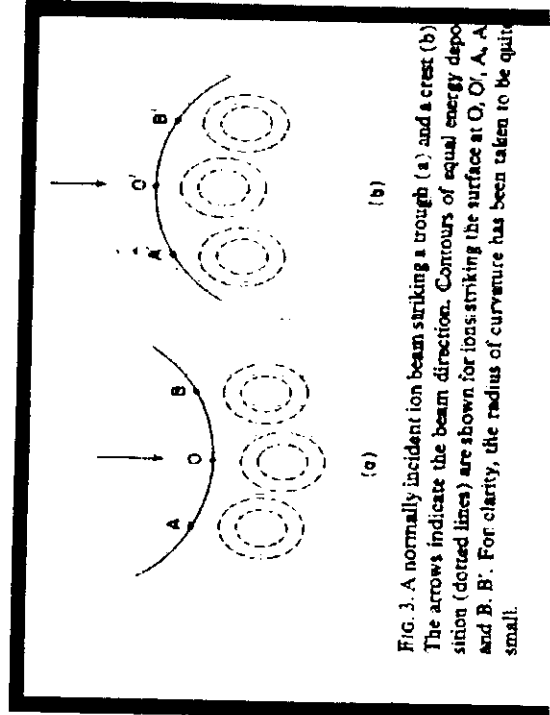
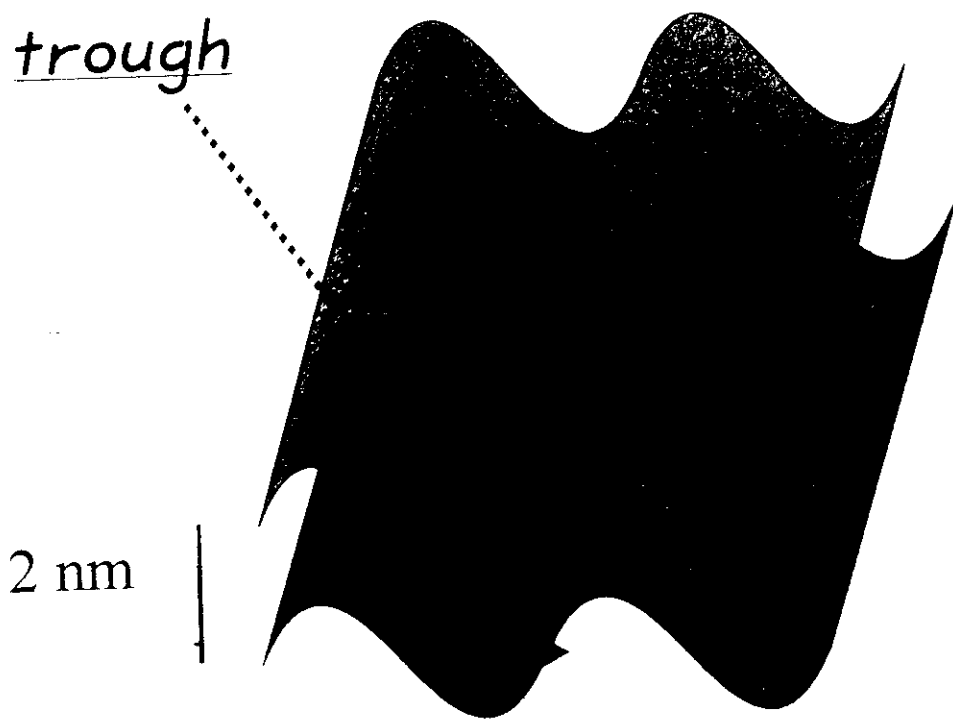


FIG. 3. A normally incident ion beam striking a trough (a) and a crest (b). The arrows indicate the beam direction. Contours of equal energy deposition (dotted lines) are shown for ions striking the surface at O, O', A, A', and B, B'. For clarity, the radius of curvature has been taken to be quite small.

The curvature-dependent effect results from the fact that power deposition which causes sputtering is maximized below the surface.

Ions incident on a peak are likely to sputter atoms from the neighboring slopes, while ions incident on a trough are likely to sputter atoms near the trough



Dynamic Scaling of Ion-Sputtered Surfaces

Rodolfo Cuerno¹ and Albert-László Barabási^{1,2}

¹*Center for Polymer Studies and Department of Physics, Boston University, Boston, Massachusetts 02215*

²*IBM T. J. Watson Research Center, P. O. Box 218, Yorktown Heights, New York 10598*

(Received 15 November 1994)

We derive a stochastic nonlinear equation to describe the evolution and scaling properties of surfaces eroded by ion bombardment. The coefficients appearing in the equation can be calculated explicitly in terms of the physical parameters characterizing the sputtering process. We find that transitions may take place between various scaling behaviors when experimental parameters, such as the angle of incidence of the incoming ions or their average penetration depth, are varied.

PACS numbers: 79.20.Rf, 64.60.Ht, 68.35.Rh

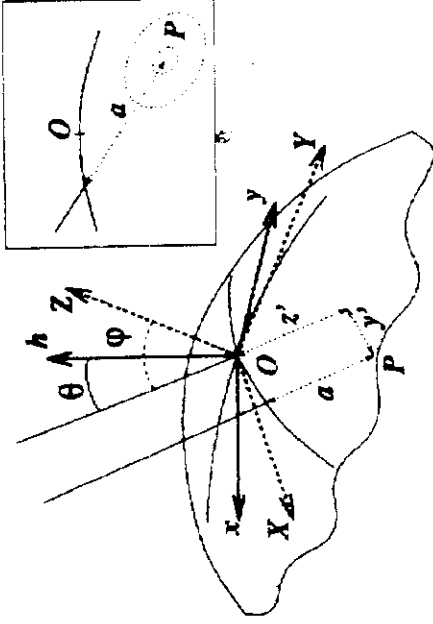
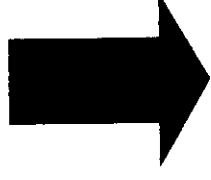


FIG. 1. Reference frames for the computation of the erosion velocity at point O . Inset: Following a straight trajectory (solid line) the ion penetrates an average distance a inside the solid (dotted line) after which it completely spreads out its kinetic energy. The dotted curves are equal energy contours. Energy released at point P contributes to erosion at O .

Average energy deposited at O

$$E(\mathbf{r}') = \frac{\epsilon}{(2\pi)^{3/2} \sigma \mu^2} \exp \left\{ -\frac{z'^2}{2\sigma^2} - \frac{x'^2 + y'^2}{2\mu^2} \right\}.$$



Normal velocity of erosion at O

$$v = p \int_{\mathcal{R}} d\mathbf{r} \Phi(\mathbf{r}) E(\mathbf{r}),$$



$$\frac{\partial h(x, y, t)}{\partial t} \cong -v(\varphi, R_x, R_y) \sqrt{1 + (\nabla h)^2},$$

$h(x, y, t)$ is measured from the initial flat configuration which is taken to lie in the (x, y) plane.

$$\frac{\partial h}{\partial t} = -v_0 + \gamma \frac{\partial h}{\partial x} + \nu_x \frac{\partial^2 h}{\partial x^2} + \nu_y \frac{\partial^2 h}{\partial y^2} + \frac{\lambda_x}{2} \left(\frac{\partial h}{\partial x} \right)^2 + \frac{\lambda_y}{2} \left(\frac{\partial h}{\partial y} \right)^2 - K \nabla^2 (\nabla^2 h) + \eta$$

Self-diffusion

$$v_0 = \frac{F}{\sigma} c, \quad \gamma = \frac{F}{\sigma} s(a_0^2 c^2 - 1),$$

$$\lambda_x = \frac{F}{\sigma} c \{ a_0^2 (3s^2 - c^2) - a_0^4 s^2 c^2 \},$$

$$\lambda_y = -\frac{F}{\sigma} c \{ a_0^2 c^2 \},$$

$$\nu_x = \frac{F}{2} a_0 \{ 2s^2 - c^2 - a_0^2 s^2 c^2 \},$$

$$\nu_y = -\frac{F}{2} a_0 c^2.$$

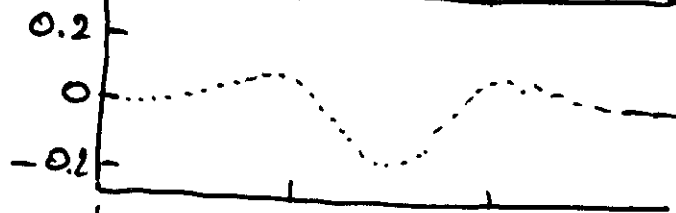
Gaussian white noise
accounting for stochastic
arrival of ions

$$\rho \nabla^2 h$$

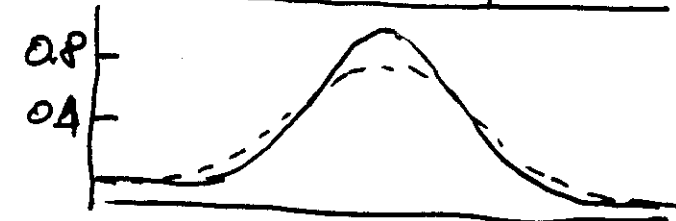
Surface Tension

$$\rho \nabla^2 h$$

$$h(x,t)$$



$$h(x, t + \Delta t)$$



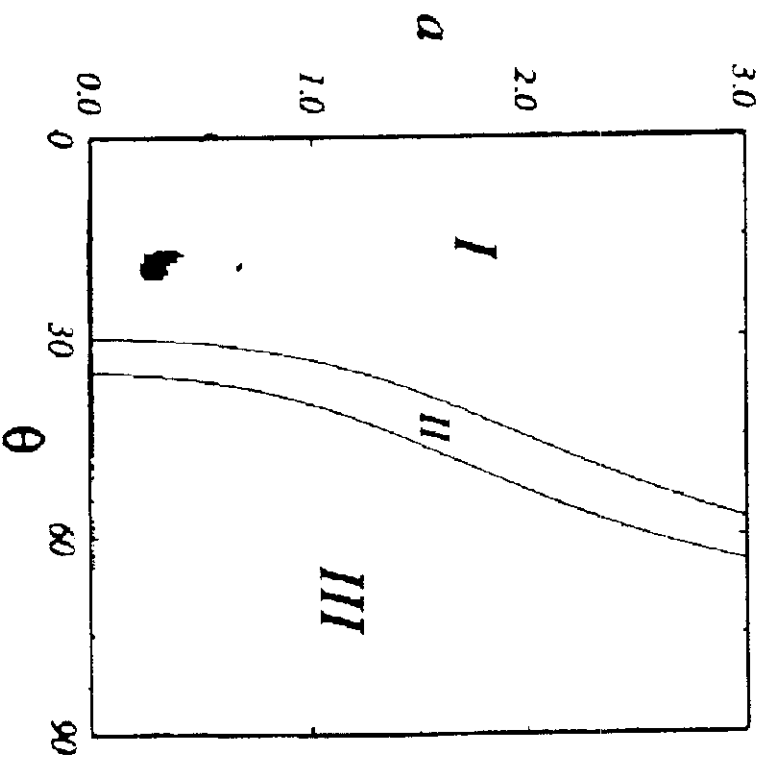


FIG. 2. Phase diagram for the isotropic case $\sigma = \mu = 1$.
 Region I: $\nu_x < 0, \nu_y < 0, \lambda_x < 0, \lambda_y < 0$; region II: $\nu_x < 0, \nu_y < 0, \lambda_x > 0, \lambda_y < 0$; region III: $\nu_x > 0, \nu_y < 0, \lambda_x > 0, \lambda_y < 0$. Here a is measured in arbitrary units and θ is measured in degrees.

Roughening Instability and Evolution of the Ge(001) Surface during Ion Sputtering

E. Chason, T. M. Mayer, B. K. Kellerman, D. T. McIlroy, and A. J. Howard

Sandia National Laboratories, Albuquerque, New Mexico 87185

(Received 21 January 1994)

We have investigated the temperature-dependent roughening kinetics of Ge surfaces during low energy ion sputtering using energy dispersive x-ray reflectivity. At 150°C and below, the surface is amorphized by ion impact and roughens to a steady state small value. At 250°C the surface remains crystalline, roughens exponentially with time, and develops a pronounced ripple topography. At higher temperature this exponential roughening is slower, with an initial sublinear time dependence. A model that contains a balance between smoothing by surface diffusion and viscous flow and roughening by atom removal explains the kinetics. Ripple formation is a result of a curvature-dependent sputter yield.

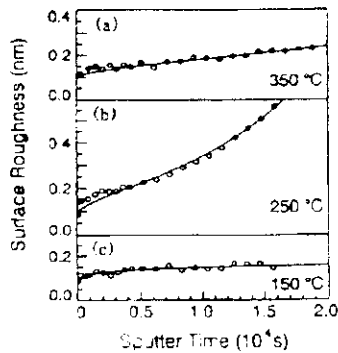


FIG. 1. Ge surface roughening kinetics at substrate temperatures of (a) 350°C, (b) 250°C, and (c) 150°C. The ion beam is 1 keV Xe with a flux of $3.2 \times 10^{13} \text{ cm}^{-2} \text{ s}^{-1}$. Solid lines are the results of model calculations based on Eq. (5).

Surface diffusion is the primary smoothing mechanism on crystalline surfaces while viscous flow is dominant for amorphous surfaces

The model of the surface evolution includes a curvature-dependent roughening term and surface transport processes which smoothen the surface. The roughening process leads to a surface instability which favors the exponential growth of a selected range of spatial frequencies

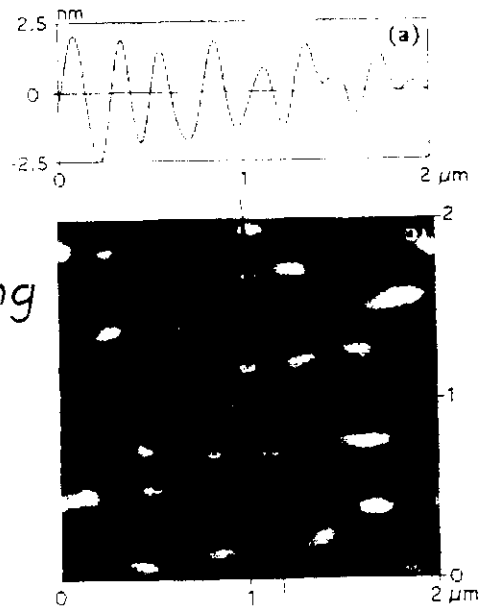


FIG. 3. (a) AFM line scan and (b) topograph of Ge surface after 1 keV Xe ion bombardment at 300°C. Sample was sputtered for 370 min with an incident flux of $4.8 \times 10^{12} \text{ cm}^{-2} \text{ s}^{-1}$. The solid line in (b) indicates the incident direction of the ion beam and the direction of the line scan in (a).

Ripple formation on amorphous carbon

Experiment :

E.A.Eklund, R. Bruinsma, J. Rudnick,
R.S.Williams PRL 67, 1759 (1991)

Theory:

VOLUME 78, NUMBER 13

PHYSICAL REVIEW LETTERS

31 MARCH 1997

Simulations of Ripple Formation on Ion-Bombarded Solid Surfaces

I. Koponen,* M. Hautala,[†] and O.-P. Sievänen

Department of Physics, University of Helsinki, P.O. Box 9, FIN-00014 Helsinki, Finland

(Received 7 October 1996)

Ripple formation on amorphous carbon surfaces bombarded by 5 keV Ar ions is studied by atomistic simulations. Sputtering is treated in detail by simulating the entire collision cascades originated by the bombarding Ar ions. Surface relaxation is described by a Wolf-Villain-type discrete model. Ripples and wavelike patterns are observed to emerge on the surface. The ripples have a well-defined wavelength and the orientation of the wave crests changes from normal to parallel to the beam, when the angle of incidence is increased from 30° to 60°, respectively. The wavelength is found to depend on the magnitude of the diffusion and orientation of the beam as predicted by the continuum theories. [S0031-9007(97)02870-6]

PACS numbers: 79.20.Rf, 64.60.Ht, 68.35.Bs

The model is based on an irreversible jumps of atoms guided by the rule to maximize the bonding or the number of the nearest neighbors.

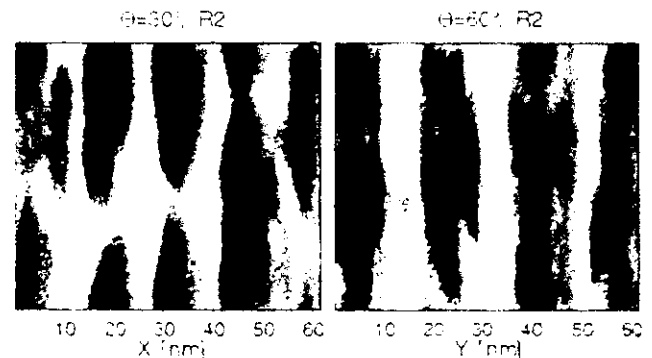


FIG. 1. Rippled simulation of surface created by 5 keV Ar ion bombardment at an angle of incidence of 30° and 60° and at a constant surface temperature. Surface relaxation is described with the Wolf-Villain model. The simulation frame is in the center of the image in the xy plane. The axes shown are in nanometers. The images show the surface profile at the end of the simulation. The dark regions represent the troughs and the light regions represent the peaks. The scale is expanded for better visibility. In the images the dark background is the trough and the light regions are the peak position.

Stochastic Model for Surface Erosion via Ion Sputtering: Dynamical Evolution from Ripple Morphology to Rough Morphology

Rodolfo Cuerno,¹ Hernán A. Makse,¹ Silvina Tomassone,² Stephen T. Harrington,¹ H. Eugene Stanley²

¹Center for Polymer Studies and Physics Department, Boston University, Boston, Massachusetts 02215

²Physics Department, Northeastern University, Boston, Massachusetts 02115
(Received 25 July 1995)

Surfaces eroded by ion sputtering are sometimes observed to develop morphologies which are either ripple (periodic) or rough (nonperiodic). We introduce a discrete stochastic model that allows us to interpret these experimental observations within a unified framework. We find that a periodic ripple morphology characterizes the initial stages of the evolution, whereas the surface displays self-affine scaling in the later time regime. Further, we argue that the stochastic continuum equation describing the surface height is a noisy version of the Kardar-Parisi-Zhang equation.

PACS numbers: 68.55.Rh, 84.60.Ht, 79.D-RL

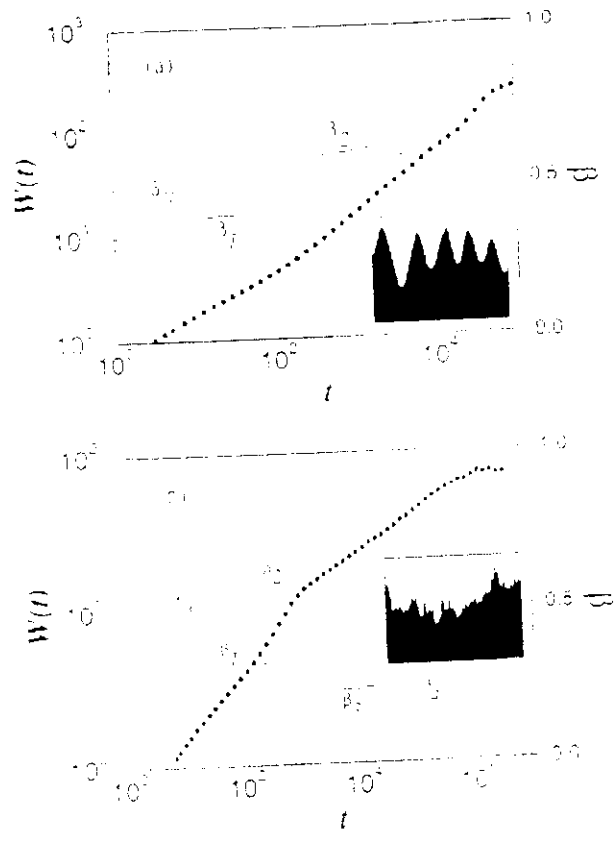
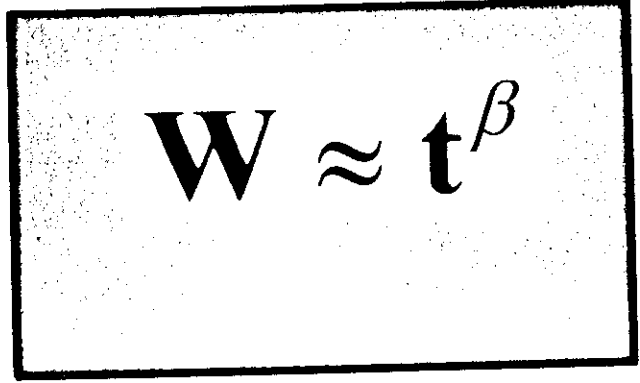
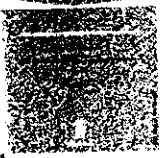


FIG. 2. Time evolution of the surface width for the cases (a) $L = 50$ and (b) $L = 2048$. The solid line is the consecutive slope of the width, showing the value of the growth exponent β in each regime. The inset shows the ripple structure of the interface at $t = 1000$. The saturation observed in $W(t)$ is due to the discreteness of the lattice; the erosion rate breaks down when the local slopes of the interface are bigger than $\pi/2$ [20]. This effect can be avoided by using a bigger box. (b) Interface width as a function of time for the full model, showing the regimes of the evolution for $L = 2048$. As in (a), the solid line is the consecutive slope. The inset shows a portion of the rough morphology at the late regime, where the self-affine scaling holds. The arrows indicate the times at which the image in (a) is displayed in Fig. 1.

surface science **DM Smilgies et al. (1997) 377.1038**



1.6	-----	-----
1.4	-----	-----
1.2	-----	-----
1.0	-----	-----
0.8	-----	-----
0.6	-----	-----
0.4	-----	-----
0.2	-----	-----
0.0	-----	-----

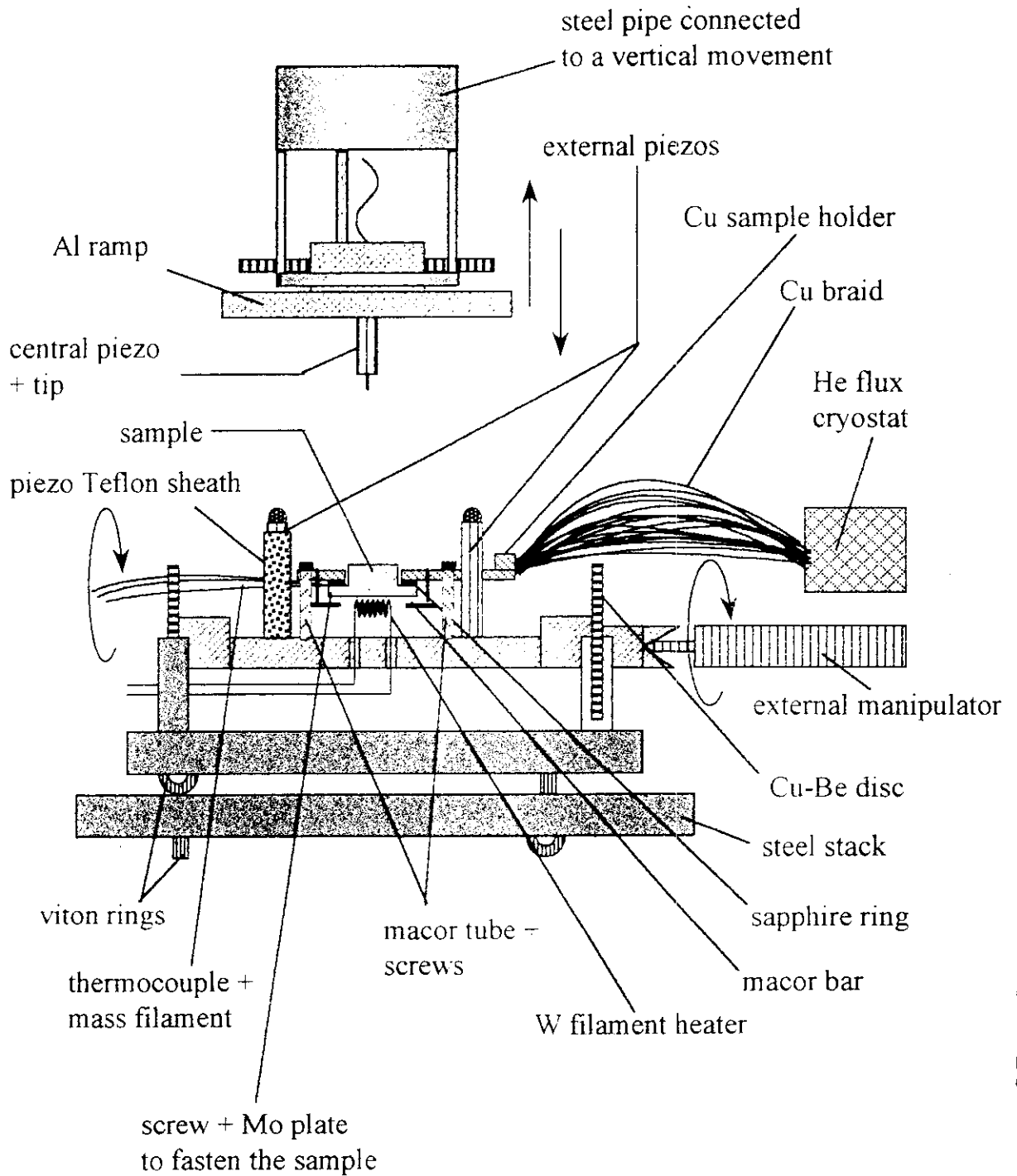
400 400 400 400 400 400

temperature (K)

scattering of Ga₂O₃

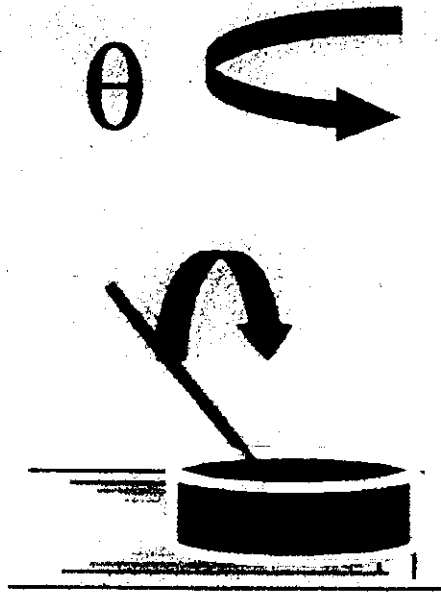
Fig. 2. Effective dynamic exponent β as a function of temperature obtained during sputtering of Ga₂O₃. The solid line is the consecutive slope of the width, showing the value of the growth exponent β in each regime. The inset shows the ripple structure of the interface at $t = 1000$. The saturation observed in $W(t)$ is due to the discreteness of the lattice; the erosion rate breaks down when the local slopes of the interface are bigger than $\pi/2$ [20]. This effect can be avoided by using a bigger box. (b) Interface width as a function of time for the full model, showing the regimes of the evolution for $L = 2048$. As in (a), the solid line is the consecutive slope. The inset shows a portion of the rough morphology at the late regime, where the self-affine scaling holds. The arrows indicate the times at which the image in (a) is displayed in Fig. 1.

STM scheme



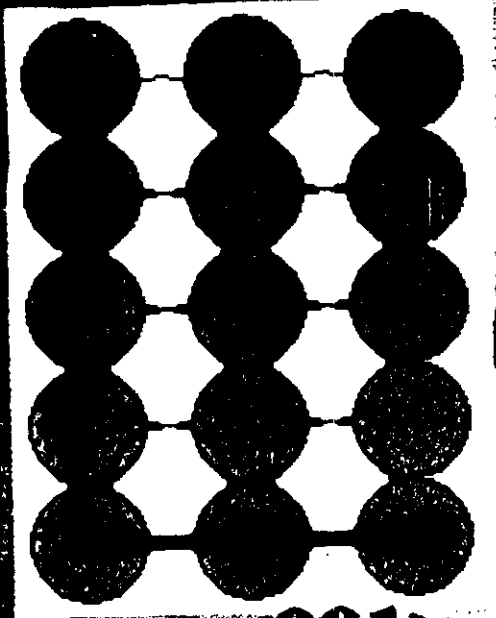
Experiment

Ar⁺



Φ

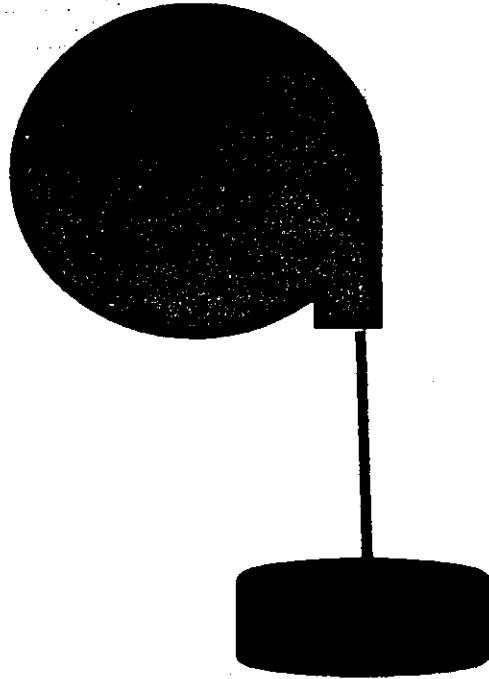
$$\Psi = \Phi t$$



<001>



600 A



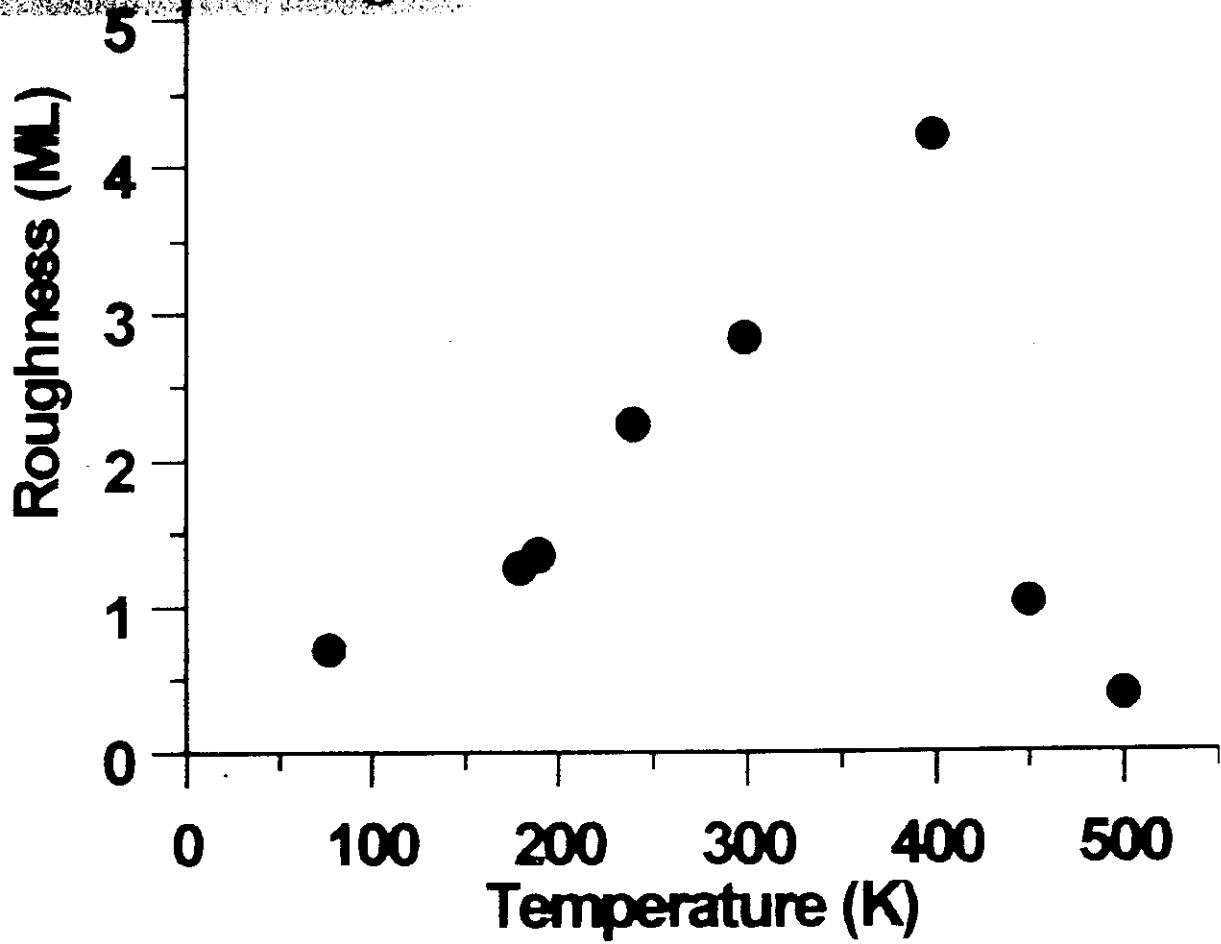
$E = 1 \text{ keV}$
 $\Phi = 0.035 \text{ ML s}^{-1}$
 $\Psi = 32 \text{ ML}$



Temperature dependence of surface roughness for Ag(100)

$$W = \sqrt{\frac{\sum_{i=1}^N (h_i - \bar{h})^2}{N}}$$

N: number of points
h_i: local surface height
 \bar{h} : surface mean height



An useful quantity to characterize the interface is the roughness W

$$W = \sqrt{\langle (h(r,t) - \bar{h})^2 \rangle}$$

where $h(\mathbf{r},t)$ is the height of the interface
 \bar{h} is the averaged height

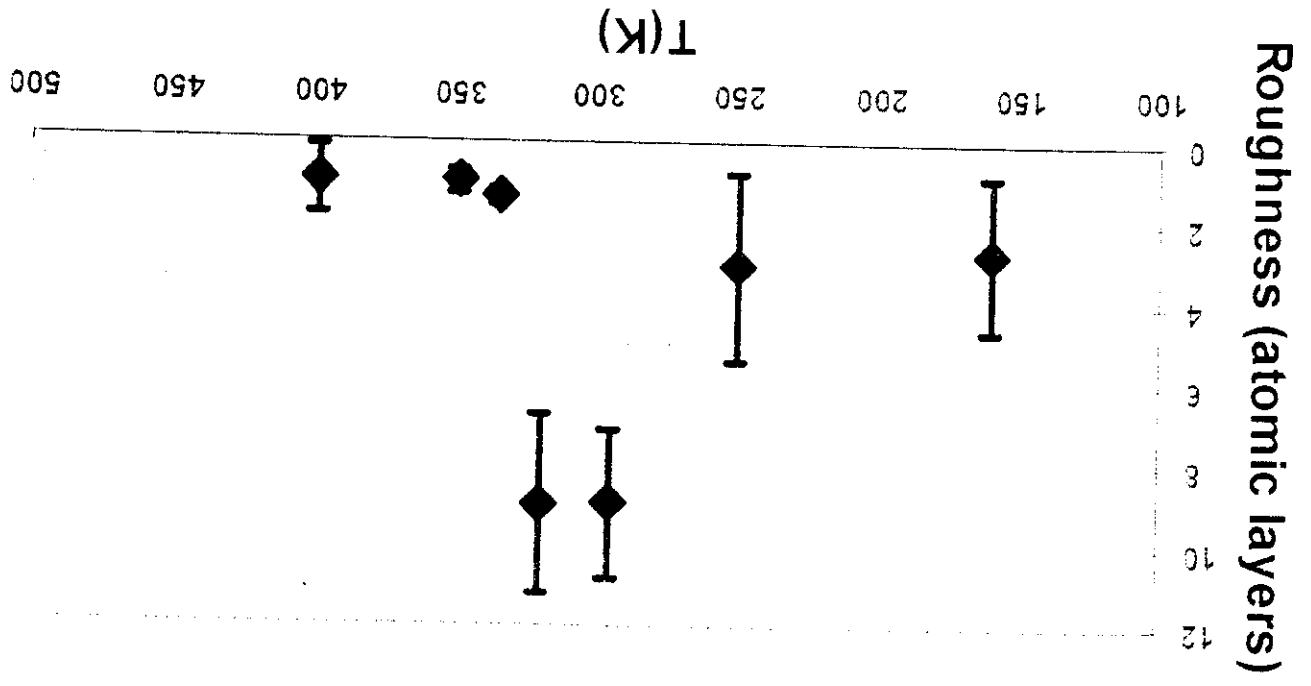
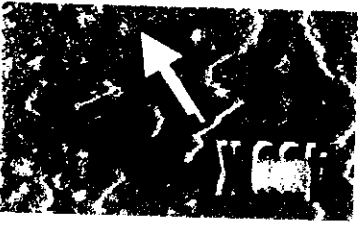
For a self-affine system

$W \propto L^\alpha$ α is the rough exponent

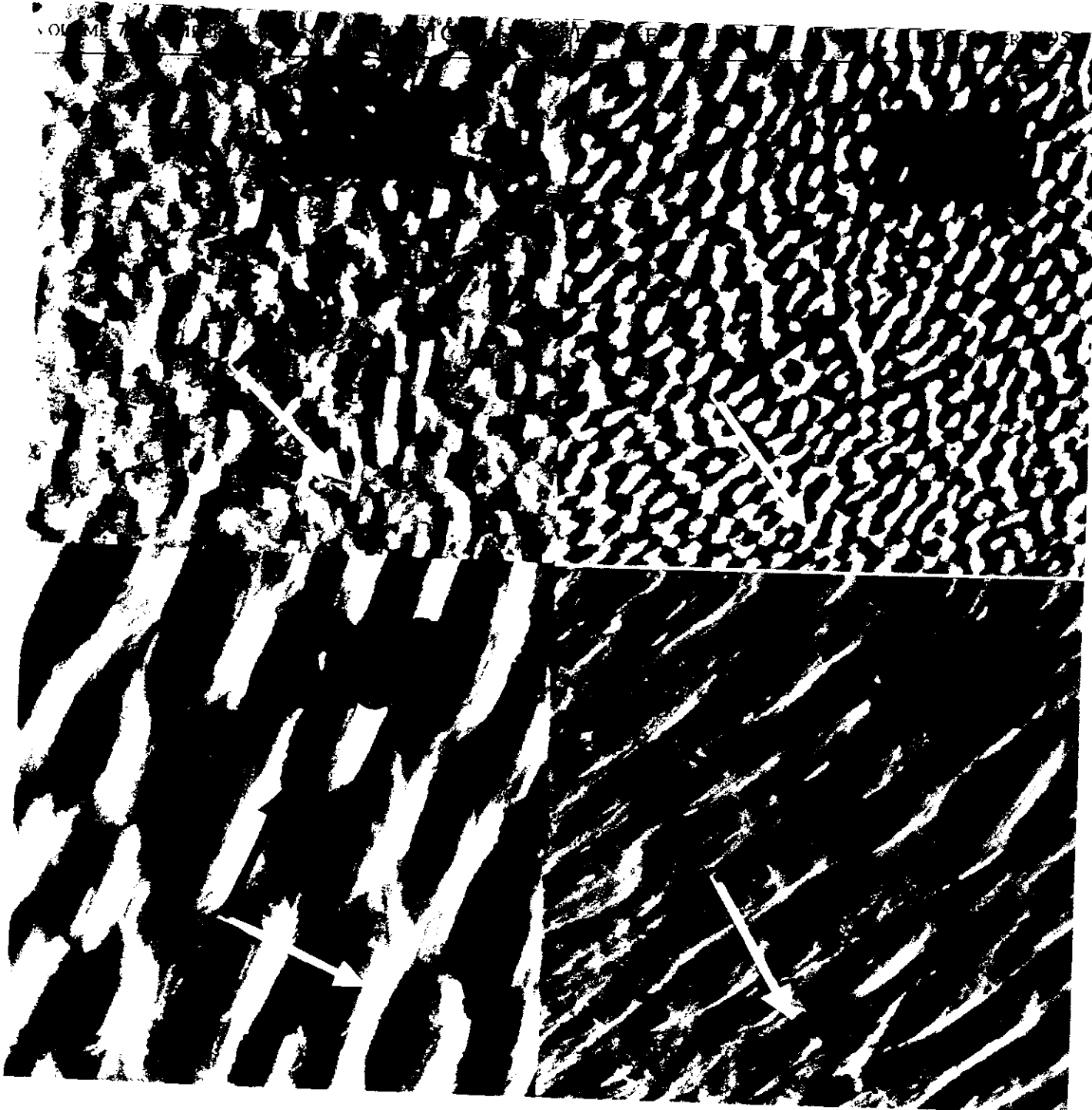
$W \propto t^\beta$ β is the growth exponent

2.4.2
 1.4.11

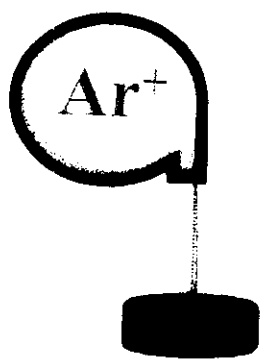
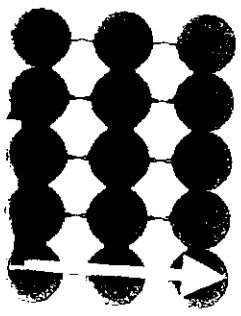
1.4.11
 2.4.2



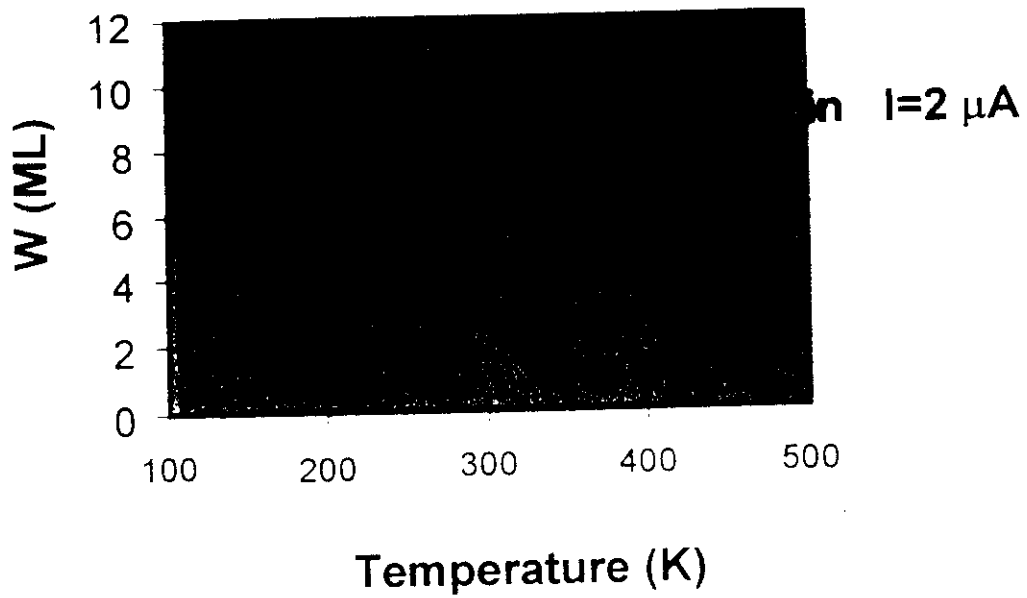
Agil



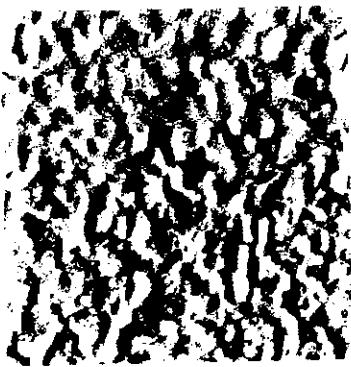
CL(110)



Roughness as a function of temperature



Cu (110)



250K

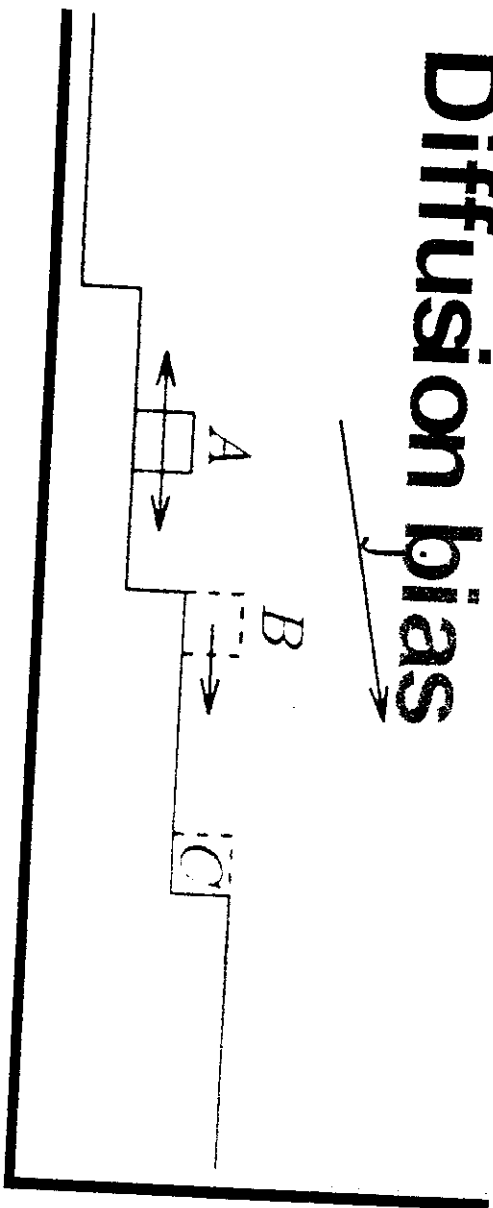


300K



350K

Diffusion bias



$m \equiv |\nabla^2 h|$ slope of the surface.

$$\rho \sim \frac{1}{m}$$

The current is proportional to the number of atoms reaching the edge of the upper step.

$$\left(-\nabla^2 h \right) + \nabla^2 \left(\nabla^2 h \right)^2 \dots$$

Continuum equation

Replace the isotropic diffusion term $-D\nabla^2(\nabla^2 h)$

for each crystallographic direction \mathbf{n} with



$$-S_n(n \cdot \nabla)^2 h - D_n(n \cdot \nabla)^4 h$$

$$S_n \propto 1 - R_n \quad R_n = \frac{\text{probability of descending a step}}{\text{probability of bounding back}} = e^{-E_{S_n}/kT}; \quad E_{S_n} \text{ Schwoebel barrier along } \mathbf{n}$$

$$D_n \propto e^{-E_{D_n}/kT} \quad \text{diffusion coefficient along direction } \mathbf{n} \quad E_{D_n} \text{ diffusion energy barrier along direction } \mathbf{n}$$

In linear approximation:

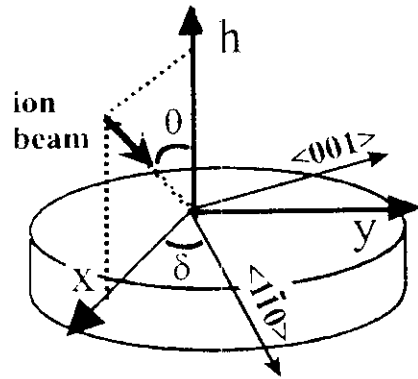
$$\frac{\partial h}{\partial t} = -v_0 + \gamma \frac{\partial h}{\partial x} + (v_x - S_{110}) \frac{\partial^2 h}{\partial x^2} + (v_y - S_{001}) \frac{\partial^2 h}{\partial y^2} + |A(E, \theta)| \nabla^2 h - D_{110} \frac{\partial^4 h}{\partial x^4} - D_{001} \frac{\partial^4 h}{\partial y^4} + \eta$$

$$\frac{\partial h}{\partial t} = -v_0 + \gamma \frac{\partial h}{\partial x} + v_x \frac{\partial^2 h}{\partial y^2} + v_y \frac{\partial^2 h}{\partial x^2} + |A(E, \theta)| \nabla^2 h - S \nabla^2 h - D \nabla^4 h + \eta$$

recoiling adatom diffusion induced by irradiation term

$$|A(E, \theta)| \nabla^2 h$$

$|A(E, \theta)|$ Depends on the energy distribution and the incidence angle



Atomic displacement term

Schwoebel term

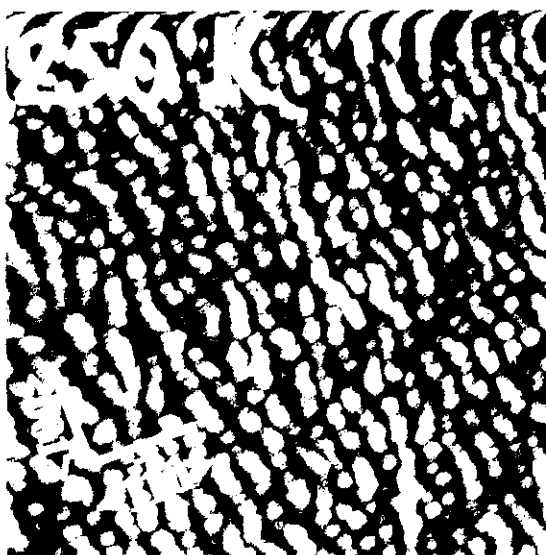
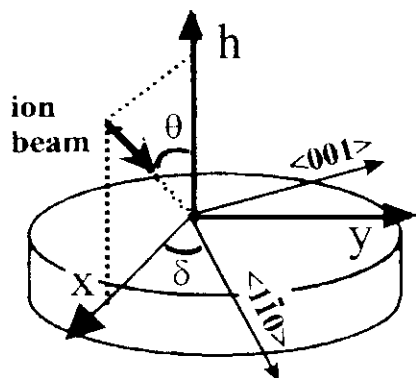
$$\frac{\partial h}{\partial t} = -v_0 + \gamma \frac{\partial h}{\partial x} + (v_x - S_{1\bar{1}0}) \frac{\partial^2 h}{\partial x^2} + (v_y - S_{00}) \frac{\partial^2 h}{\partial y^2}$$

$$+ |A(E, \theta)| \nabla^2 h + \frac{\lambda_x}{2} \left(\frac{\partial h}{\partial x} \right)^2 + \frac{\lambda_y}{2} \left(\frac{\partial h}{\partial y} \right)^2$$

$$- D_{1\bar{1}0} \frac{\partial^4 h}{\partial x^4} - D_{001} \frac{\partial^4 h}{\partial y^4} + \eta$$

Anisotropic surface diffusion

Cu(110), $\theta = 0^\circ$



$T = 180K$

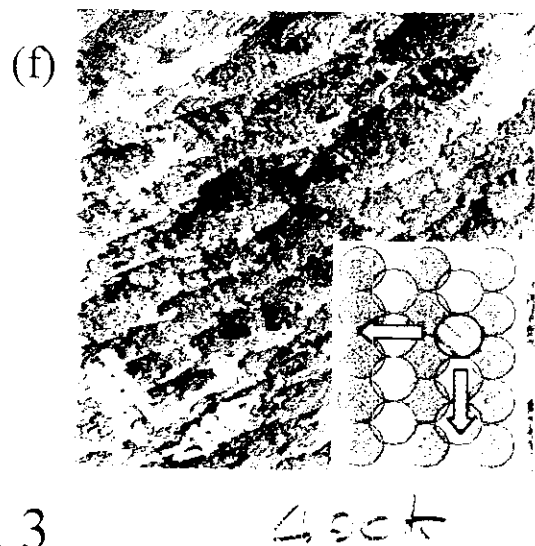
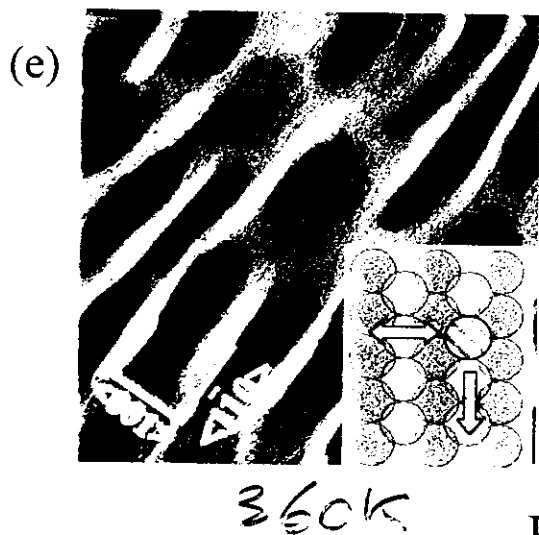
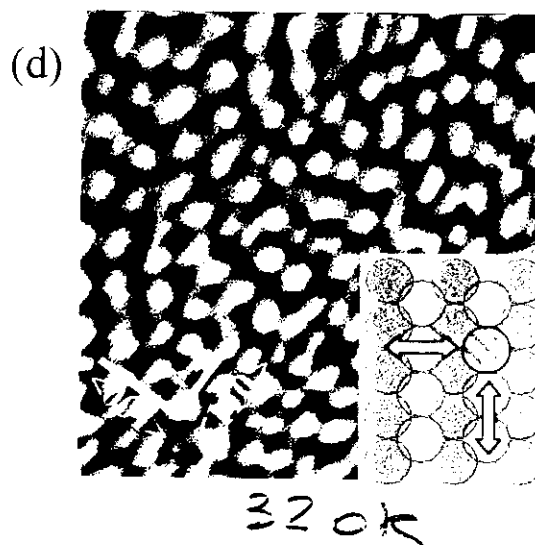
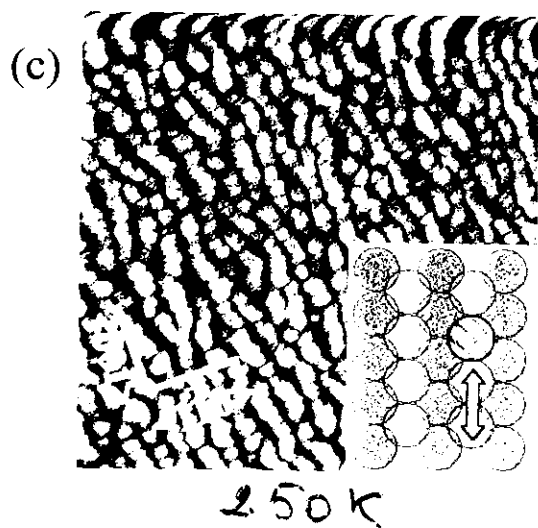
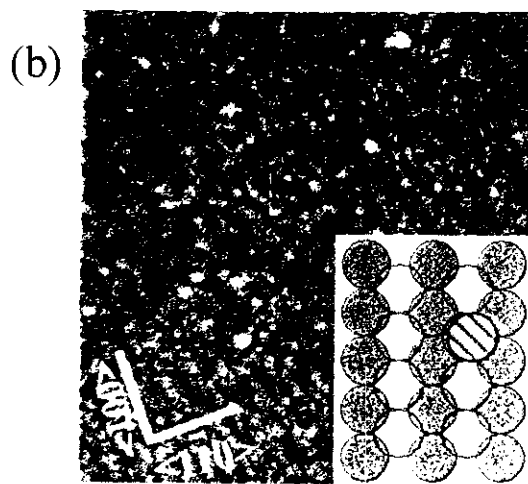
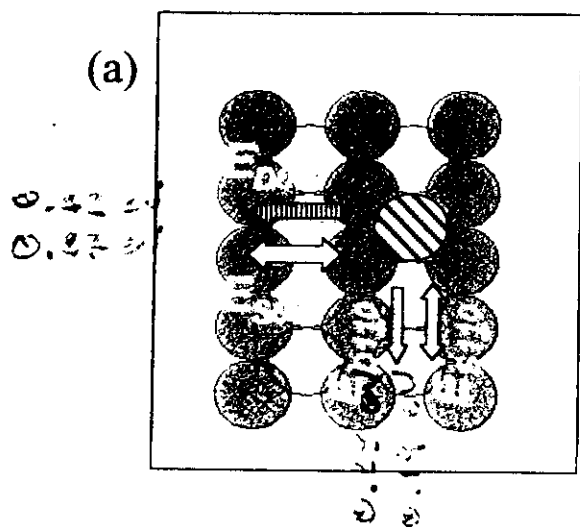
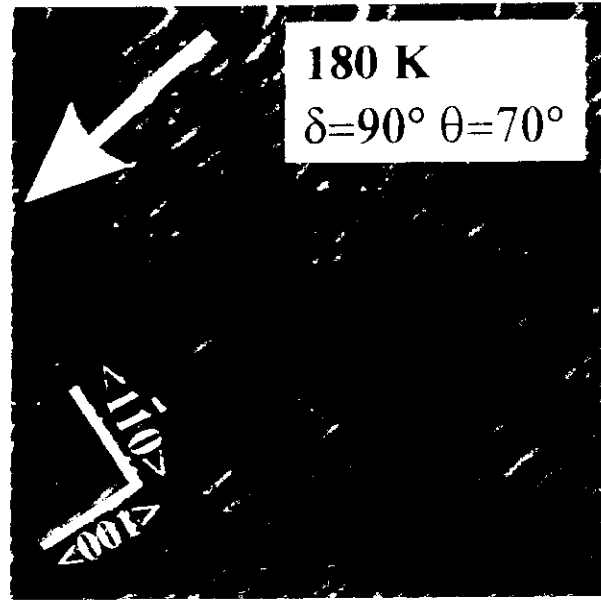
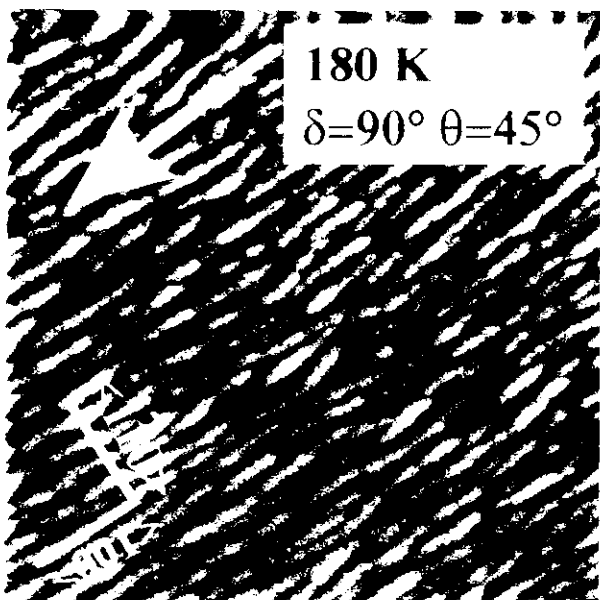
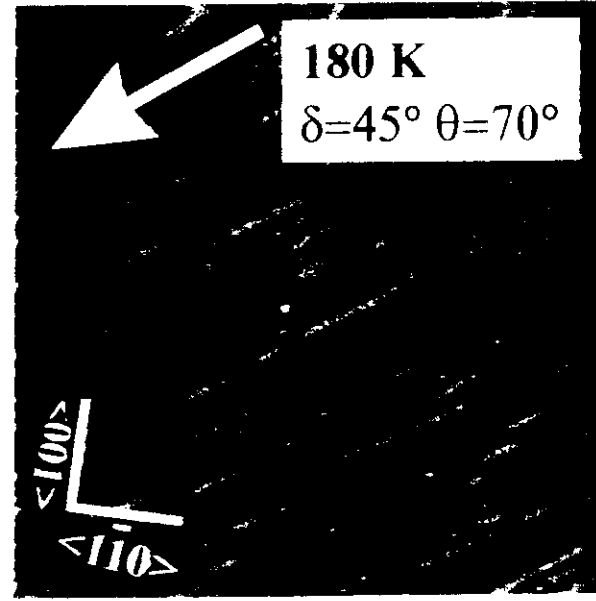
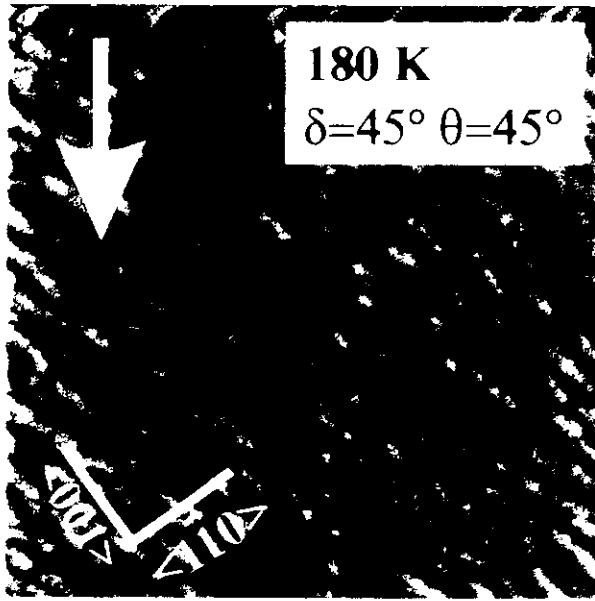
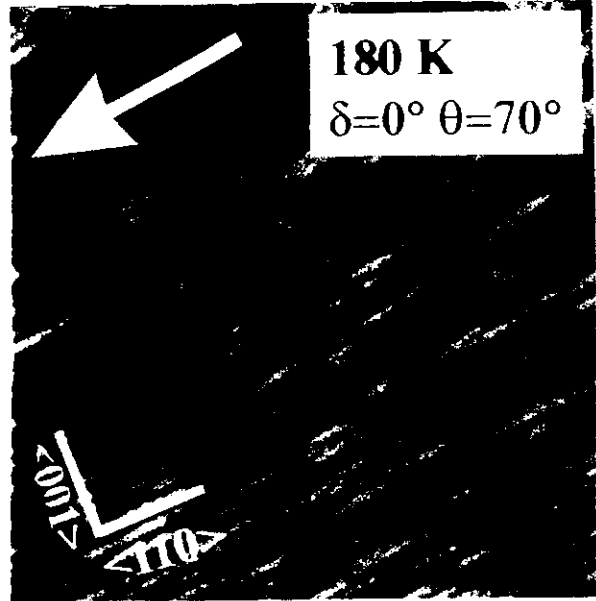
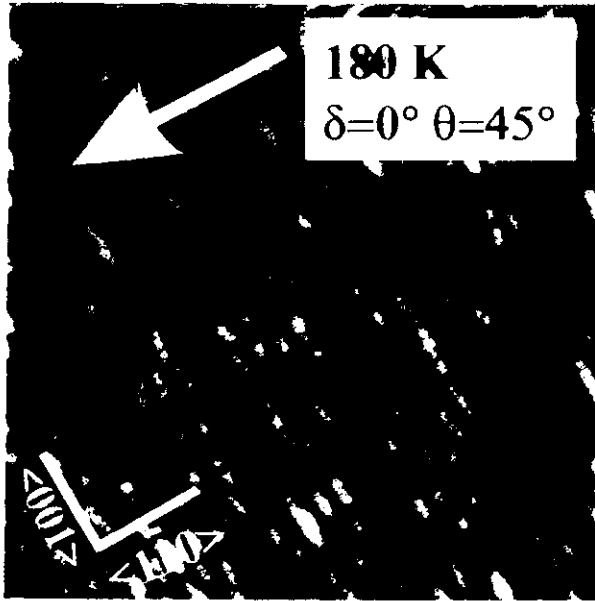


Fig. 3

100
200
300
400
500



Cu(110)

$T=180\text{K}$

$\Theta > 0^\circ$

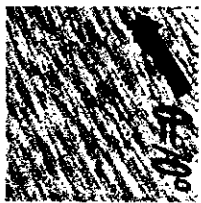
$$\delta = 0^\circ \quad \frac{\partial h}{\partial t} = -v_0 + \gamma \frac{\partial h}{\partial x} + (v_x - S_{110}) \frac{\partial^2 h}{\partial x^2} + (v_y - S_{100}) \frac{\partial^2 h}{\partial y^2} + |A(E, \Theta)| \nabla^2 h - D_{110} \frac{\partial^4 h}{\partial x^4} - D_{001} \frac{\partial^4 h}{\partial y^4} + \eta$$

$$\Theta = 45^\circ \quad v_x - S_{110} < v_y < 0$$



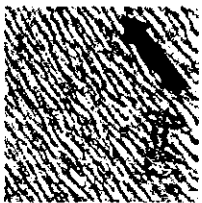
$$v_y < v_x - S_{110}$$

$$\Theta = 70^\circ \quad v_y < 0 < v_x \quad \text{and}$$



$$\delta = 90^\circ \quad \frac{\partial h}{\partial t} = -v_0 + \gamma \frac{\partial h}{\partial x} + (v_y - S_{110}) \frac{\partial^2 h}{\partial y^2} + v_x \frac{\partial^2 h}{\partial x^2} - D_{110} \frac{\partial^4 h}{\partial y^4} + \eta$$

$$\Theta = 45^\circ \quad v_x < v_y < 0 \quad \text{and}$$



$$|v_y - S_{110}| > |v_x|$$

$$\Theta = 70^\circ \quad v_y - S_{110} < 0 < v_x$$



$$\frac{\partial h}{\partial t} = -v_0 + \gamma \frac{\partial h}{\partial x}$$

Erosion term

$$\frac{\partial^2 h}{\partial x^2} + \nu \frac{\partial^2 h}{\partial y^2}$$

$$\frac{\nu}{2} \left(\frac{\partial h}{\partial x} \right)^2 + \frac{\nu}{2} \left(\frac{\partial h}{\partial y} \right)^2$$

$$-K \nabla^2 (\nabla^2 h)$$

$$+\eta$$

non-linear term

Diffusion term

Gaussian noise term

The time evolution of the interface can be described by a continuum equation (Cuerno & Barabasi PRL k1995)

Atomic displacement term

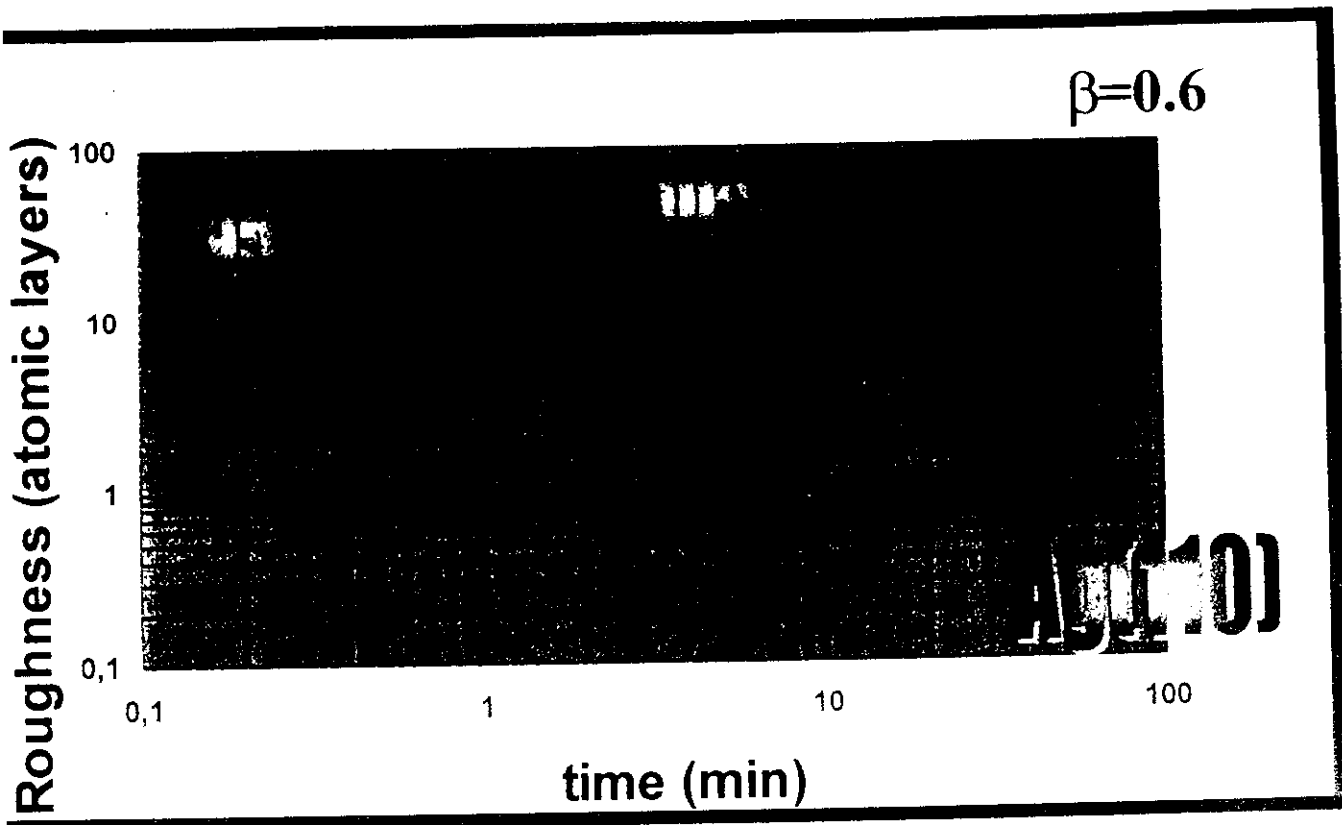
$$\frac{\partial h}{\partial t} = -v_0 + v \frac{\partial h}{\partial x} + (v_x - S_{110}) \frac{\partial^2 h}{\partial x^2} + (v_y + S_{001}) \frac{\partial^2 h}{\partial y^2}$$

Schwoebel terms

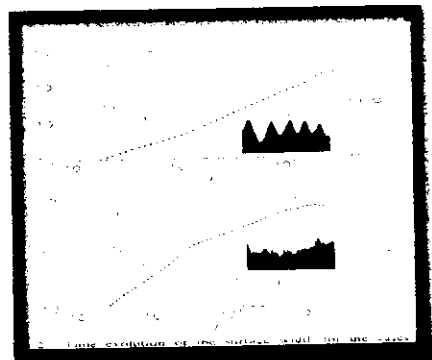
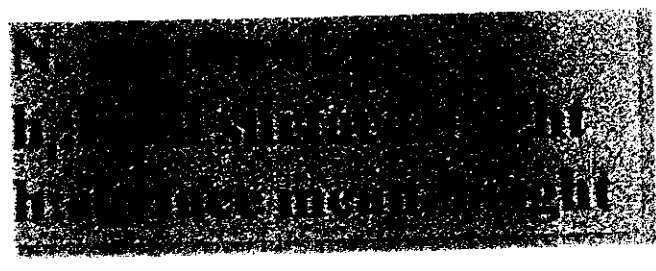
$$+ |A(E, \theta)| \nabla^2 h + \frac{\lambda_x}{2} \left(\frac{\partial h}{\partial x} \right)^2 + \frac{\lambda_y}{2} \left(\frac{\partial h}{\partial y} \right)^2$$

$$- D_{1D} \frac{\partial^4 h}{\partial x^4} - D_{00} \frac{\partial^4 h}{\partial y^4} + \eta$$

Anisotropic surface diffusion



Roughness

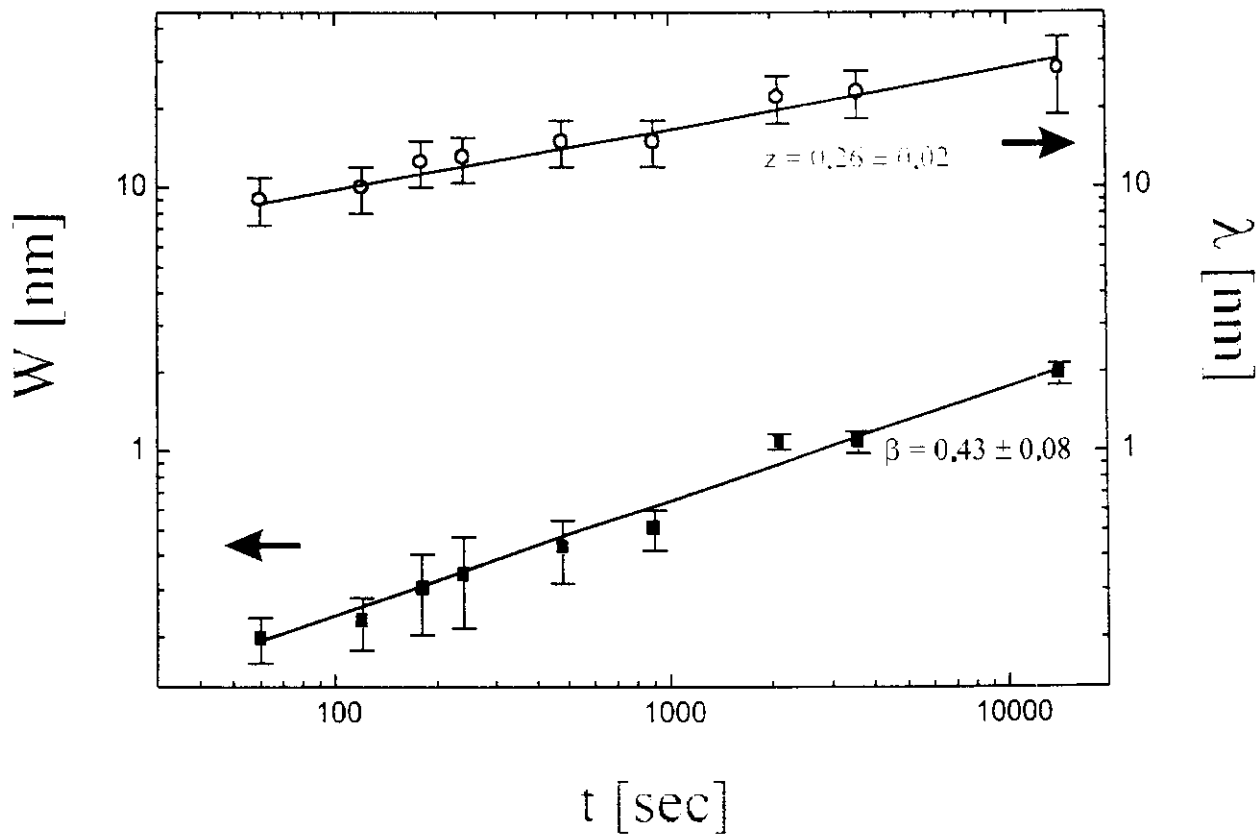


Scaling law

Family, Phys. Rev. E 168 (1993), 561

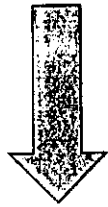
Time evolution of roughness and ripple wavelength

$T = 180 \text{ K}, \theta = 45^\circ, \delta = 0^\circ, \Phi = 0.09 \text{ ML/sec}$



Two scaling laws: $\lambda \propto t^{0.25}$, $W \propto t^{0.43}$

The wavelength grows as $\lambda \propto t^{0.25}$, with the same scaling law observed in MBE growth when a Schwoebel barrier is present cfr. Fe/Fe(001), Cu/Cu(001)



in sputtering process the presence of a Schwoebel barrier is important to determine the final morphology

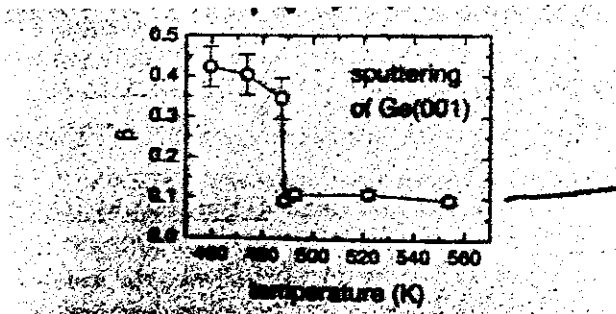
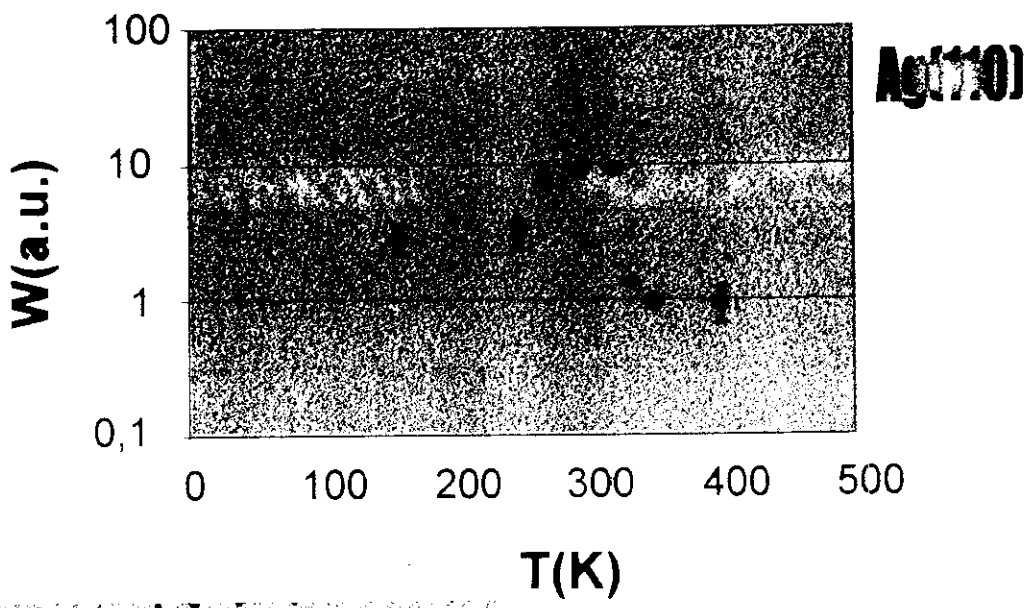
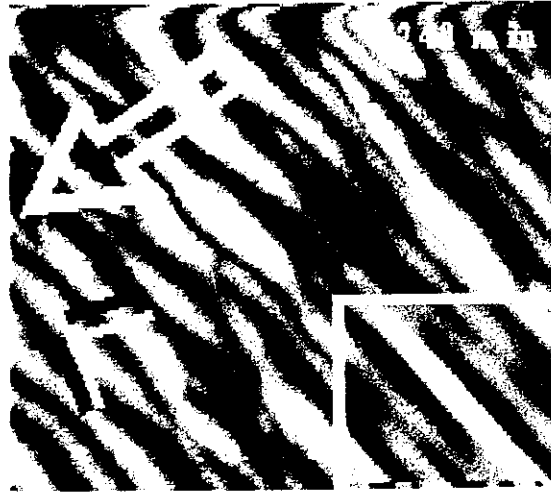
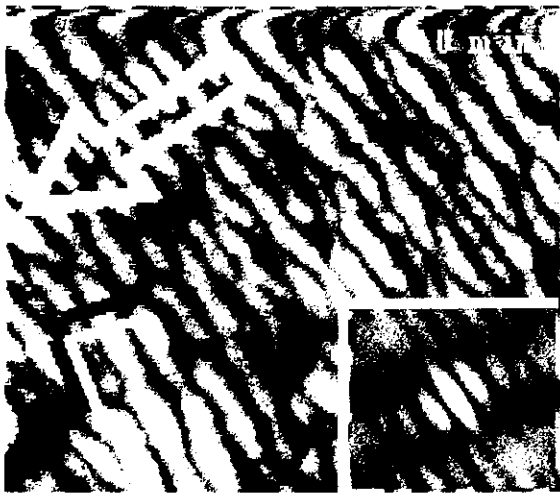
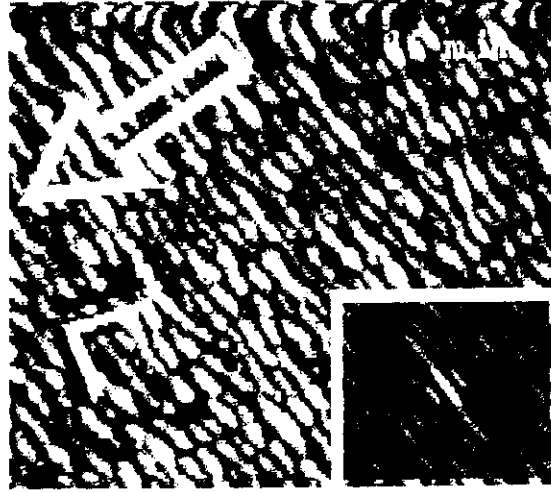
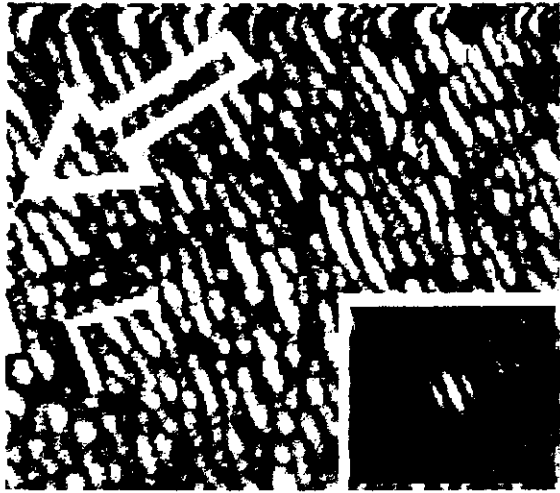
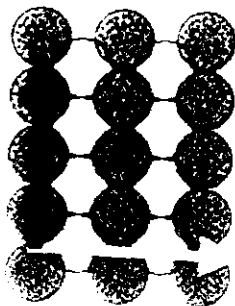


Fig. 2. Dynamic scaling exponent β versus sample temperature during sputtering of a Ge(001) surface, as derived from the data points in Fig. 1. For $\beta \approx 0.4$ random fluctuations dominate the dynamic behavior, whereas for $\beta \approx 0.1$ there is a dynamic equilibrium between fluctuations and surface diffusion. We attribute the jump of the β value at 493 K to a dynamic phase transition.





After 140 min



... has been
... and holes
reflecting the surface symmetry

- ⇒ Pt(111) , Michely & Comsa (1993)
- ⇒ Cu(111) , Naumann et al. (1997)
- ⇒ Cu(001) , Ritter et al. (1996)
- ⇒ Fe films , Krim et al. (1993)

This difference is due to the prevalence of the smoothing terms (i.e. diffusion terms) and then it should be possible to induce a ripple structure by lowering the temperature

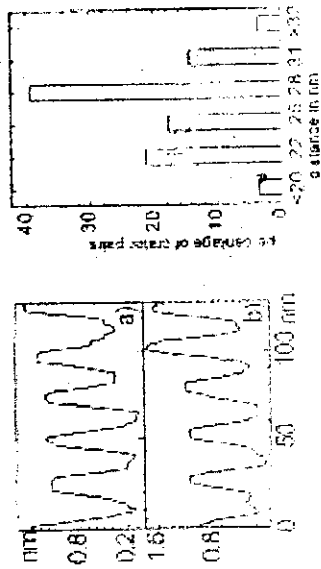
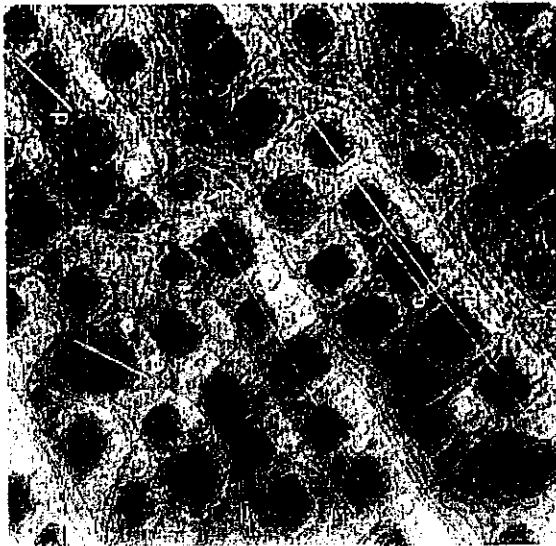


Fig. 3. Top: μ -EDS ($200 \times$, 1.500 kV , 5.0 nA) image of the specimen at 4K from the surface plane in Fig. 8. The distance was $5 \mu\text{m}$. Right: Fe content of the grain pairs (a) and the percentage of grain pairs (b) vs. distance. The error bars represent the standard deviation. The line shows the average Fe content of the grain pairs and the percentage of the grain pairs. The bars show the percentage of the grain pairs.

M. Ritter, M. Stindtman, M. Farle, K. Baberschke



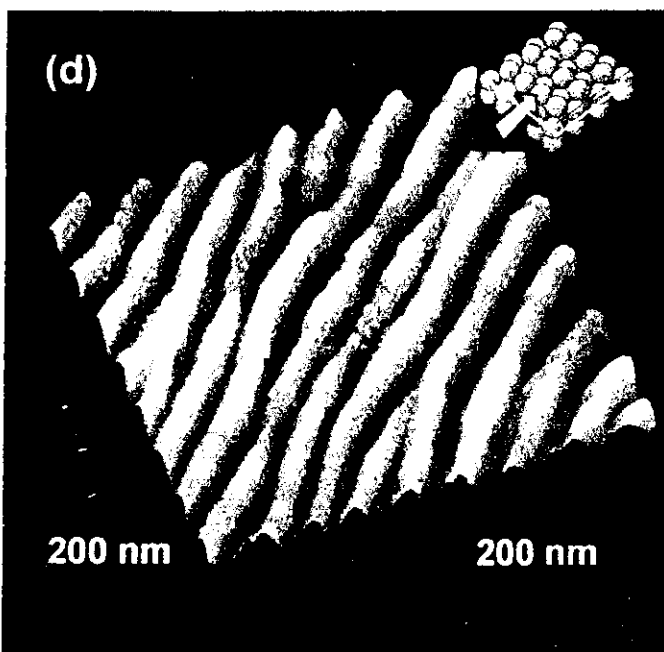
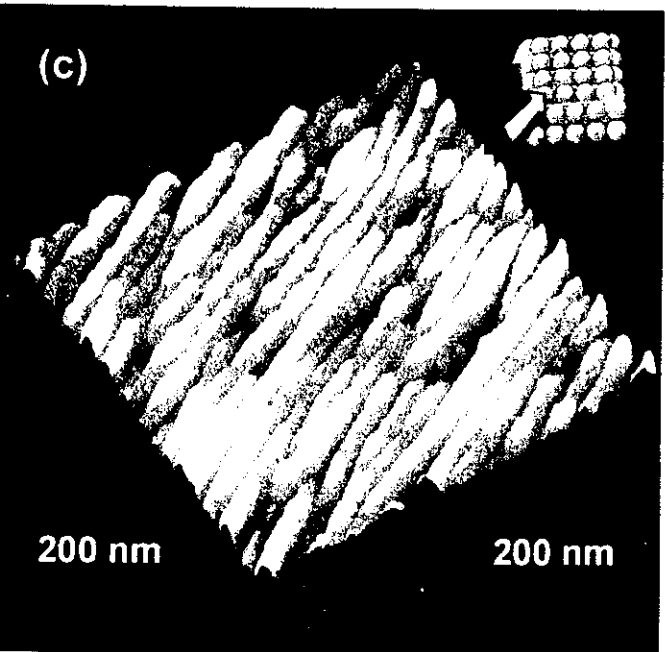
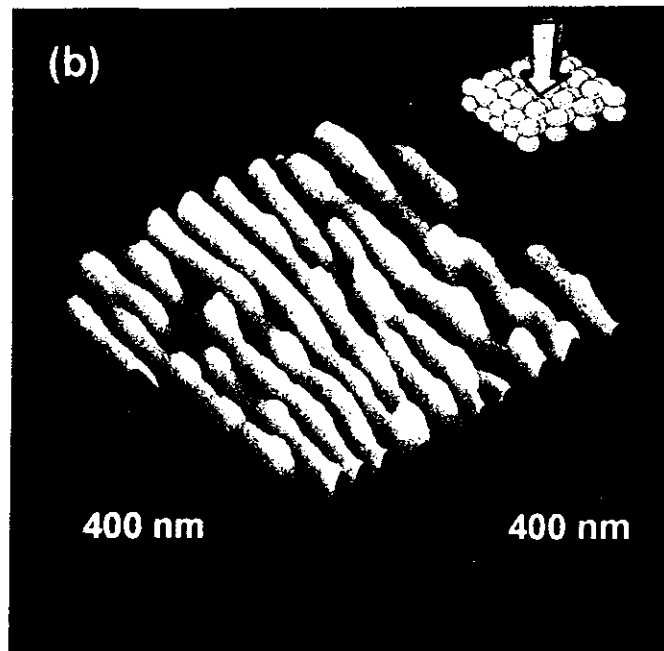
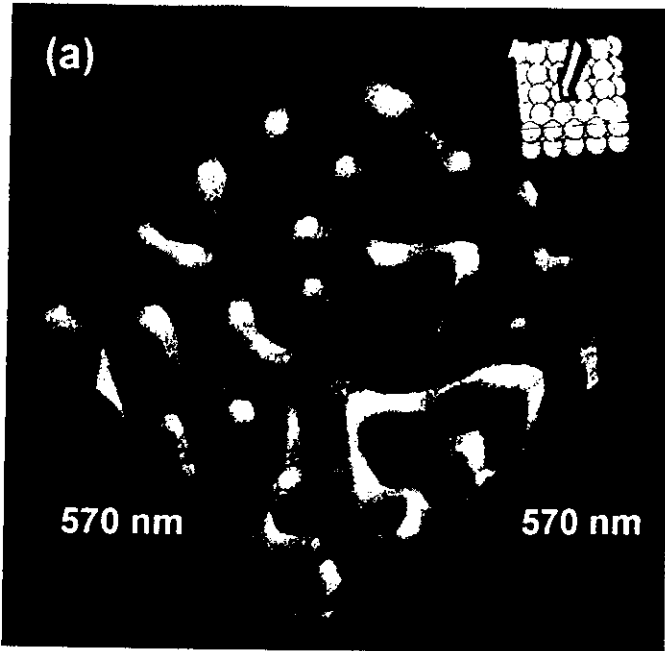


Figure 1

1
2
3
4
5
6
7
8
9
10
11
12
13
14
15
16
17
18
19
20
21
22
23
24
25
26
27
28
29
30
31
32
33
34
35
36
37
38
39
40
41
42
43
44
45
46
47
48
49
50
51
52
53
54
55
56
57
58
59
60
61
62
63
64
65
66
67
68
69
70
71
72
73
74
75
76
77
78
79
80
81
82
83
84
85
86
87
88
89
90
91
92
93
94
95
96
97
98
99
100